Fundamental equations linking methylation dynamics to maximum lifespan in mammals

Steve Horvath[1,2,3], Joshua Zhang[1], Amin Haghani[1,3], Zhe Fei[2,4]

Affiliations
[1]Department of Human Genetics, University of California, Los Angeles
[2]Department of Biostatistics, University of California, Los Angeles
[3]Altos Labs, San Diego, California
[4]Department of Statistics, University of California, Riverside

Abstract

Many studies have investigated the connection between the rate of change in diverse molecular markers and maximum lifespan across species. We describe a framework to address doubts that the rate of change in any biomarker displays a trivial inverse relation to lifespan. We leverage this framework on two comprehensive methylation datasets. The first connects the rate of change in blood methylation to the lifespan of 93 dog breeds. The second associates the rate of change in distinct chromatin states with the maximum lifespan of 125 mammalian species. We show how methylation levels in selected chromatin states shift with age across the lifespan. Our research reveals three significant outcomes: First, a reciprocal relationship exists between the rate of methylation change in bivalent promoter regions and maximum lifespan. Second, the association between age and average methylation within these bivalent promoter regions bears no relation to maximum lifespan. Third, the rate of methylation change in young animals is related to that in old animals. Our mathematical derivations draw connections between these findings. A substantial part of our mathematical framework for analyzing maximum lifespan can be applied to other molecular assessments as well. Overall, our study demonstrates that epigenetic aging rates in specific chromatin states exhibit an inverse relationship with maximum lifespan.

Introduction

A fundamental question in biology is why closely related species, such as mammals, exhibit significant differences in maximum lifespans (also referred to as maximum longevity or simply longevity). Years of research have outlined the ecological traits associated with maximum lifespan. In short, maximum lifespan is closely linked to an organism's ability to avoid predation, such as having a large body size, the capacity to fly, or the skill to burrow underground [1, 3, 10, 12, 15, 16, 19]. The rate of living theory suggests that the faster an organism's metabolism, the shorter its lifespan. This theory was initially proposed by Max Rubner in 1908, following his observation that larger animals lived longer than smaller ones, and that these larger animals had slower metabolisms. Rubner's rate of living theory, which was once accepted, has now largely been debunked. This shift in perception is due to the application of modern statistical methods which account for the effects of both body size and phylogeny. When these factors are appropriately adjusted for, there is no correlation between metabolic rate and lifespan in mammals or birds [15, 16]. Nonetheless, contemporary adaptations of the original rate of living theory have emerged. Many articles have explored the relationship between the rate of change in various molecular markers and maximum lifespan. Specifically, maximum lifespan has been connected to the rates of change in telomere attrition [5, 11, 25, 45, 46, 49], somatic mutations [6, 8, 35, 40, 44], and cytosine methylation [21, 32, 34].

The strong correlation between maximum lifespan and the rate of change in various factors (telomeres, somatic mutations, methylation) raises the possibility that these relationships might merely be artifacts resulting from the definition of the rate of change. In other words, the strong correlation with maximum lifespan could be a simple mathematical consequence stemming from the calculation of rates

of change per year. To address this concern, we introduce a framework that links the rate of change in a biomarker to maximum lifespan. We show that any biomarker positively correlated with age in multiple species will exhibit an inverse relation with maximum lifespan. Thus considerable care must be taken to avoid biases deriving from the definition of the rate of change. We study the relationship between methylation dynamics across the life course and maximum lifespan in two data sets from the Mammalian Methylation Consortium [22]. The first dataset includes blood methylation data from 93 different dog breeds, while the second dataset involves methylation data from 125 mammalian species.

Results

Rate of Change in Methylation in Dog Breeds

Dog breeds exhibit a striking range of lifespans, with some breeds living up to twice as long as others. A prior study involving two dog breeds indicated an inverse relationship between methylation change rate and breed-specific lifespan [32]. Here we examine the connection between methylation change rate and the lifespans of dog breeds using a substantially larger dataset: $N = 742$ blood samples from 93 different dog breeds [27]. For later applications, we will use the more abstract term "stratum" instead of "dog breed". The definition of Average Rate of Change in Methylation (AROCM) depends on the age interval and the set of cytosines. The AROCM quantifies the rate or gradient of age-related changes in a set of cytosines across samples from a given stratum. Within each stratum (dog breed) and given an age range $[\ell, u]$, we assume there are n (blood) samples from the stratum within the age range. Let the methylation matrix be represented as:

$$\mathbf{M}_{n\times p} = (CG_{ij})(i = 1, 2, .., n; j = 1, 2, .., p), \tag{1}$$

where rows represent (blood) samples and columns represent a set of p CpGs (e.g., CpGs located in a specific chromatin state). For the i-th sample, the average methylation value $Methyl$ is defined as:

$$Methyl_i = \frac{1}{p}\sum_{j=1}^{p} CG_{ij}. \tag{2}$$

To enable comparisons with other aging biomarkers, we define the scaled methylation value as:

$$ScaledM_i = \frac{Methyl_i - Mean(Methyl_i)}{\mathrm{SD}\,(Methyl_i)}, \tag{3}$$

within each stratum where the Mean and SD are taken over samples $i = 1, 2, .., n$. We define the Average Rate of Change in Methylation ($AROCM^{(s)}$) in the s-th stratum as the coefficient estimate β_1 resulting from the univariate linear regression model:

$$ScaledM_i = \beta_0 + \beta_1 Age_i. \tag{4}$$

The term "average" in AROCM reflects that $Methyl$ was defined as the average value across cytosines (equation 2) in a specific chromatin state (Methods). For the dog data, we focused on the 552 CpGs located in universal chromatin state BivProm2+ (Methods). We define relative age as the ratio of age to maximum lifespan:

$$R \doteq \frac{Age}{Lifespan}. \tag{5}$$

Using equation (20), we obtain:

$$\mathrm{AROCM} = \frac{\mathrm{Cor}(Methyl, Age)}{\mathrm{SD}\,(R)}\frac{1}{Lifespan}. \tag{6}$$

Equation (6) posits a significant concern that the inverse association between the rate of change and maximum lifespan could be a trivial outcome of selecting CpGs that have a positive correlation with age. To address this, we pursued several approaches. Initially, we established a mathematical framework connecting rates of change to lifespan (Methods). Next, we conducted simulation studies clearly showcasing this bias source as a significant concern. Finally, we refrained from pre-filtering

CpGs based on their age correlations, instead opting to mitigate the bias by defining the rate of change with respect to chromatin states rather than individual CpGs (Methods). In practice, the calculation of AROCM and the age correlation $\mathrm{Cor}(Age, Methyl)$ can be compromised by influential outliers, narrow age range, and low sample sizes. For example, our dog data set had two major limitations. First, the number of dogs per stratum/breed varied significantly (from $n = 2$ for English Setter to $n = 95$ for Portuguese Water Dog). Second, uneven age ranges were ascertained per stratum: the relative ages $R^{(s)}$ of breed Otterhound ranged from 0.06 to 0.14 while $R^{(s)}$ ranged from 0.06 to 0.73 for breed Beagle. To mitigate these limitations, we executed two primary steps. Firstly, we removed strata with sparse samples, as outlined in the Methods section. More crucially, we brought forward two new definitions (refer to equation 25 in Methods) for tailoring the AROCM and the age correlation, aligned with a power of the standard deviation of relative ages R:

$$Adj.AROCM^{(s)} \doteq AROCM^{(s)} \mathrm{SD}\,(R^{(s)})^{1-p}, \tag{7}$$
$$Adj.\mathrm{Cor}(Methyl^{(s)}|R^{(s)}, p) \doteq \frac{\mathrm{Cor}(R^{(s)}, Methyl^{(s)})}{\mathrm{SD}\,(R^{(s)})^{p}}.$$

Note, the adjustment process involves the power parameter p, the selection of which is governed by a criterion detailed below. Assuming that $Adj.\mathrm{Cor}(Methyl|R, p)$ does not correlate with lifespan on the logarithmic scale, we can derive the following fundamental relationship:

$$Adj.AROCM^{(s)} \approx \frac{constant}{Lifespan^{(s)}}. \tag{8}$$

The assumption, which underlies the fundamental relationship, guides the criterion for choosing the power p: select p to minimize the coefficient of variation in the adjusted age correlation (equation 44, Methods). According to this guideline, $p = 0.1$ is an apt choice for our dog methylation data (Supplementary Figure S1).

As anticipated, the adjusted age correlation does not correlate with lifespan (Figure 2b). Our mathematical derivations (equations 8 and 42) validate that this independence signifies a potent negative correlation between Adj.AROCM and lifespan on the logarithmic scale, which indeed is the case ($r = -0.75$, Figure 1b, Supplementary Table 1).

Using adjusted versions of the AROCM bears two benefits. Firstly, it often boosts the data signal ($r = -0.75$ for the adjusted AROCM versus $r = -0.36$ for the unadjusted AROCM, Figure 1a,b). Secondly, it aids in deriving formulas for constants of proportionality (equation 42). For instance, we notice $constant = 1.02$ in equation 8).

We also identify positive correlations between AROCM and average breed weight (Figure 1e,f), which is predictable since breed weight inversely correlates with breed lifespan.

In conclusion, these studies reveal that a) the AROCM has a negative correlation with breed lifespan, and equivalently b) the positive age correlation does not connect to lifespan. These findings also extend to the broader question of mammalian maximum lifespan as demonstrated in the following.

Mammalian Methylation Data and chromatin states

Recent investigations have revealed a connection between the rates of methylation change and the maximum lifespan of mammals [32]. In the present study, we revisit this question utilizing a comprehensive dataset from the Mammalian Methylation Consortium [22, 33]. These data are well suited for comparative aging rate studies, as the mammalian array platform provides a high sequencing depth at CpGs, which are highly conserved across mammalian species [2]. We maintained the same definitions as our dog dataset, though strata were classified by species and tissue types within species. In order to derive reliable AROCM estimates, we removed outlying species/tissue strata using stringent criteria (Methods). For analysis of the complete age range $[0, Lifespan)$, we scrutinized $S = 229$ distinct species/tissue strata. We first ascertained AROCMs in all species-tissue strata (Equation 6) and amalgamated them by species for all 54 chromatin states identified on the mammalian array (Supplementary Table 2). To constitute a species-level AROCM metric, we calculated the median across tissue types:

$$\mathrm{AROCM}species = \mathrm{Median}(\mathrm{AROCM}species, tissue). \tag{9}$$

Given that AROCM estimates may exhibit a non-linear relationship with the inverse of maximum lifespan, we used the Spearman correlation between species AROCM and $1/L$. The Spearman correlation

coefficients of the chromatin states varied from -0.44 (ReprPC4-) to 0.66 (BivProm1+, BivProm2+) (Figure 3a, Supplementary Table 2). The most prominent positive correlation between AROCM and maximum lifespan was noticed for BivProm2+, where 194 out of 229 species-tissue strata yielded a positive correlation (Supplementary Table 2). In the subsequent discussions, we concentrate on the mean methylation $Methyl$ pertaining to the 552 CpGs within the chromatin state BivProm2+, unless specified otherwise. Similar outcomes can be observed for chromatin states BivProm1+, ReprPC1+, among others.

Non-linear relationship across the life course

Mean methylation versus age in various example species-tissue strata and age range is illustrated in Figure 3d-f). In numerous species-tissue strata, we notice a non-linear relationship between the scaled methylation value $ScaledM$ (Equation 3) and relative age R (Figure 4). The non-linear behavior between $ScaledM$ and age presents a mathematical challenge when estimating AROCM. However, this can be addressed by dividing the age range into segments that can be approximated by a linear relationship (Figure 3d-f). Roughly linear relationships can be observed when focusing on either young animals (defined by $R < 0.1$) or older animals ($R \geq 0.1$). For instance, in humans, we designated the young stratum by $R < 0.1$, corresponding to $Age < 12.2$ years, while the older stratum was defined as $Age \geq 12.2$. To alleviate potential concerns about these threshold choices, we conducted extensive sensitivity analyses that demonstrated the robustness of our results concerning different thresholds of $0.2, 0.3, \ldots, 0.9$.

We determined AROCM in relation to three distinct chromatin states: BivProm2+, BivProm1+, and ReprPC1+. All three chromatin states reveal that a) AROCM is higher in young animals compared to older ones, but there is a strong correlation between AROCM in young and old animals ($r > 0.78$, Figure 5).

Age correlation does not relate to lifespan

The correlation between $Methyl$ and Age, denoted as $\mathrm{Cor}(Methyl, Age)$, correlates with the standard deviation of relative age (Pearson correlation r=0.26 in all species tissue strata, r=0.31 across species, Supplementary Figure S2a,b). Our simulations suggest the unexpected positive correlation between $\mathrm{Cor}(Methyl, Age)$ and $\mathrm{SD}\,(R)$ stems from strata differences in sample size and relative age distribution (Supplementary Figure S3).

The adjusted age correlation $Adj.Cor(M|R, p)$ (equation 25, $p = 0.25$, Supplementary Figure S1b)has two appealing attributes compared to the unadjusted age correlation. First, it no longer depends on $\mathrm{SD}\,(R)$ (Supplementary Figure S2d,e). Second, its variability of $Adj.Cor$ is less than that of $\mathrm{Cor}(Methyl, Age)$ across species (QCOD=0.137 vs 0.189, Figure 7). The average $Adj.Cor(Methyl, Age)$ is nearly 1.0 across species (Mean = 1.04, Supplementary Figure S2f).

We find that $\mathrm{Cor}(Methyl, Age)$ assumes similar values for long and short lived species, e.g. Median Cor(Methyl,Age)=0.51 for humans, 0.58 for humpback whale, 0.62 for Asian elephant, 0.66 for mouse, 0.67 for brown rat, 0.69 for prairie vole. Neither $\mathrm{Cor}(Methyl, Age)$ nor $Adj.Cor$ depend on species' lifespans (Figure 7).

To further characterize the relationship between age correlation and maximum lifespan, we assigned each species to one of 5 groups defined by maximum lifespan, e.g. $Lifespan < 10$ years, or lifespan in $[10, 20)$, $[20, 25)$, $[25, 40)$, or > 40. We find that $\mathrm{Cor}(Methyl, Age)$ does not relate to lifespan group according to a trend test (Figure 8a,b). The non-monotone trends are preserved between $Adj.Cor$ and the lifespan groups (Figure 8c,d). Similarly, we find no relationship between lifespan and $\mathrm{Cor}(Methyl, Age)$ when the latter is defined with respect to young (Supplementary Figure S4) or old animals (Supplementary Figure S5).

Adjusted AROCM equals the inverse of maximum lifespan

Since $Adj.Cor$ does not correlate with lifespan and its coefficient of variation is low, $Adj.AROCM$ follows an inverse relationship with maximum lifespan (equation 8 and Proposition 4). On the log scale, adjusted AROCM exhibits a strong negative correlation with maximum lifespan (r=-0.927 for adjusted AROCM, and r=-0.919 for unadjusted AROCM Figure 6a,c). Since the adjusted correlations take on values close to 1.0 (Figure 7b), equation 42 implies that the adjusted AROCM is roughly equal to $1/Lifespan$ (equation 8). This is indeed the case as can be seen from Figure 6b,d.

Strong negative correlations between lifespan can be observed when AROCM is defined with respect to young animals only ($R < 0.1$) or old animals only ($R \geq 0.1$, Supplementary Figure S6). Since maximum lifespan is positively correlated with average age of sexual maturity and gestation time, we find that both variables correlate strongly with AROCM as well (Supplementary Figure S7).

Adult weight does not confound the relationship between AROCM and lifespan

Body size (e.g. measured using average adult body mass or adult weight) is a major determinant of maximum lifespan—with larger animals living, on average, longer than smaller ones [7, 9, 15, 30, 37, 39, 42]. Adult weight is often a confounding factor in comparative studies of maximum lifespan [24, 37, 41]. To address this concern about confounding, we carried out several analyses to demonstrate that adult weight does not explain the observed relationships between AROCM and maximum lifespan. First, we demonstrate that the correlation between log(AROCM) and log(Weight) is much weaker than that observed for maximum lifespan ($r = -0.65$ for average weight, Supplementary Figure S8a, versus r=-0.85 for maximum lifespan, Figure 6a). Second, we fit several multivariate regression models between AROCM, maximum lifespan and adult weight (Table 1).

$$\begin{aligned} M1 &: \log(L) \sim \log(AROCM) + \log(Weight) \\ M2 &: \log(AROCM) \sim \log(L) + \log(Weight). \end{aligned} \tag{10}$$

When lifespan is regressed on AROCM and weight on the log scale, both AROCM and weight are highly significant (model M1, Table 1). When AROCM is regressed on lifespan and weight, all on the log scale, lifespan remains highly significant while weight is not (model M2, Table 1). Overall, these results demonstrate that adult weight has only a weak effect on the relationship between lifespan and AROCM.

Effect of tissue type on the relation between AROCM and lifespan

Most proliferating tissue types have similar values of $\mathrm{Cor}(Methyl, Age)$ but slightly lower correlations can be observed for non-proliferating tissues such as the cerebellum, cerebral cortex, skeletal muscle, and heart when looking at all samples irrespective of age (Supplementary Figure S9). To carry out a formal analysis of the effect of tissue type, we added indicator variables for tissue type as covariates to multivariate regression models that explored the relationship between AROCM and lifespan:

$$\begin{aligned} M3 &: log(AROCM) \sim \log(L) + \log(Weight) + Brain, \\ M4 &: log(AROCM) \sim \log(L) + \log(Weight) + Brain + Skin + Liver + Muscle + Tail, \end{aligned} \tag{11}$$

where Model 4 added indicator variables for several tissue types. Both model 3 and model 4 allow insights into the potential tissue differences in AROCM estimates, as detailed estimates can be found in Table 1. After including $\log(L)$ as the covariate, only liver tissue had a significant (positive) association with $log(AROCM)$, (p=0.03, Table 1).

Phylogenetic effects

The shared genetic, behavioral, and ecological traits among related species, inherited from common ancestors, can create non-random associations or 'phylogenetic signals'. Ignoring these phylogenetic relationships can lead to false correlations or overlook real ones [18, 24, 37]. Upon adjusting for phylogenetic relationships, the previously mentioned associations persist, albeit with weaker correlation coefficients. In the case of the dog methylation data, we observed substantial positive associations in the phylogenetically independent contrasts (PICs [18]) of AROCM and breed lifespan (refer to Supplementary Figure S10). Here, we recorded a correlation of -0.26 ($p = 0.018$), and for Adjusted AROCM, a correlation of -0.64 ($p = 7.3 \times 10^{-11}$).

Moving on to the mammalian data, we again found significant positive associations in PICs of AROCM and maximum lifespan (refer to Supplementary Figure S11). Correlations for this dataset were $r = -0.2$ ($p = 0.03$) for AROCM, -0.35 ($p = .00013$) for Adjusted AROCM, and -0.23 ($p = .022$) for Adjusted Old AROCM. Collectively, these findings indicate a connection between the rate of methylation change in bivalent promoter regions and maximum lifespan, which holds even after phylogeny adjustment.

Discussion

Calculating the rate of change for a biomarker is generally challenging due to various reasons. To begin with, the rate of change relies on the underlying age range, as the rate in young animals might be higher than that in older animals (Figure 3d-f). More broadly, the rate of change is dependent on age distribution and sample size. Ideally, a study focusing on the rate of change should encompass hundreds of species, a large number of animals per species (hundreds of animals per species), and a consistent distribution of relative age (e.g., uniform distribution of relative age). However, this is not feasible in practice. To tackle the limitations of data ascertainment, we introduce adjusted versions of the rate of change and the Pearson correlation. Our adjustment formula for the ROC aims to address biases stemming from imperfect datasets. The formula introduces an "adjustment factor" (a power of the standard deviation of relative age) for the Pearson correlation coefficient or, equivalently, the rate of change estimate. We derived our adjustment formula through simulation studies and empirically validated it using our empirical data. The relative age R, defined as the ratio of age to maximum lifespan, is critical for disentangling the relationship between rates of change and maximum lifespan. In many real datasets, the standard deviation of relative age, $\mathrm{SD}\,(R)$, varies across species due to uneven sampling, which may primarily include young or old animals in some species. This variability can dilute the signal between the rate of change and maximum lifespan, as well as affect $\mathrm{Cor}(Methyl, Age)$, as evidenced in our simulation and empirical studies. Adjusting for $\mathrm{SD}\,(R)$ amplifies the inherent biological signal in both areas. Our adjustment formulas counter biases from inconsistent $\mathrm{SD}\,(R)$ values due to uneven species ascertainment or diverse sample sizes. Applying these formulas to the methylation data allowed us to present fundamental equations that link the rate of change in methylation in specific chromatin states (e.g. bivalent regulatory regions) to maximum lifespan in mammals.

The mathematical formalism was presented in order to address two long-standing questions in biology. Why do dog breeds differ markedly in terms of lifespan? Why do similar species, like mammals, have noticeably different maximum lifespans? Here we are addressing these questions from the perspective of the rate of change in cytosine methylation across the life course (from womb to tomb) and in specific age groups (e.g. young animals only). Prior studies have linked the rate of change in methylation to maximum lifespan in smaller samples of mammalian species [21, 32, 50]. Previous studies established a strong correlation between methylation rate changes and mammalian lifespan. We build upon this through a) a mathematical framework to set underlying assumptions, b) a unique measurement platform, the mammalian methylation array, offering high sequencing depth in conserved cytosines [2], c) larger sample sizes from our Mammalian Methylation Consortium, and d) highlighting biases from the rate of change's mathematical definition. We sidestepped potential biases from age-related biomarker selection and instead focused on chromatin states. Strong correlations between AROCM and lifespan are only found in certain chromatin states such as bivalent promoters (Figure 3a). In alternate chromatin states, the correlation with lifespan is either not present or even reversed (See Supplementary Figure S12). In a similar vein, the correlation between mammalian lifespan and AROCM is not significant when employing all 8970 CpGs that correspond to both eutherians and marsupials (Supplementary Figure S13). These findings collectively underscore the significance of selecting an appropriate chromatin context for defining the AROCM. Bivalent chromatin states generally exhibit low methylation levels in most tissues and species and are bound by polycomb repressive complex 2 (PRC2) [33]. Many previous articles, including our pan-mammalian aging studies, have shown target sites of PRC2 gain methylation with age in most species and tissues [33, 38]. A simple and fundamental equation links the adjusted rate of change in bivalent chromatin regions to the inverse of maximum lifespan (equation 8). It is important to note that equation (8) does not involve hidden parameters. Our study strongly suggests that careful definition and measurement of both $Adj.AROCM^{(s)}$ and $L^{(s)}$, the choice of power p, and the interval of relative age will result in an actual equality:

$$Adj.AROCM^{(s)} = \frac{1}{L^{(s)}}. \tag{12}$$

Our mathematical framework shows that equation (12) is a mathematical consequence from another major finding from our study: the Pearson correlation between methylation levels in select chromatin states and age, $\mathrm{Cor}(Methyl, Age)$ does not depend on maximum lifespan. In particular, the age correlation in short-lived species will be similar to that in long-lived species. While we do not call the age correlation an "invariant," our studies show that it does not relate to maximum lifespan

across mammals (Figures S5, 6). Previous research in humans has indicated that the rate of change during development surpasses that during postnatal development [17, 26]. Our thorough investigation corroborates this finding for a majority of mammalian species (Figure 5). Additionally, our expansive dataset empowers us to demonstrate the correlation between the rate of change in young and old animals (Figure 5). This latter discovery can be understood from two perspectives: mathematical and biological. In mathematical terms, it is a result (equation 45) of the continuous changes in cytosine methylation levels at particular locations, from development through to old age. In fact, we offer explicit formulas that describe the monotonically increasing relationship between methylation and age across the life course (equation 46 and equation 47). Future versions of these equations might require modifications to accommodate for a potential rejuvenation phase early in development [29]. From a biological standpoint, the connection between $AROCM_{young}$ and $AROCM_{old}$ reinforces deterministic theories of aging, suggesting a link between developmental changes and those occurring in later life [4, 13, 14, 20, 28].

Our research has multiple limitations, which stem from the inherent challenges in reliably calculating a rate of change. A single influential outlier can undermine the rate of change estimate. Additionally, a limited age range poses a problem, as estimating a rate requires a reasonably broad age range. Insufficient sample sizes exacerbate the aforementioned challenges. To tackle these issues, we developed an outlier removal algorithm. Without this algorithm, the empirical data aligns far less with the mathematical formulas (Supplementary Figure S14). Other limitations relates to potential confounders such as body size, tissue type, and phylogenetic relationships. Our multivariate model analysis partially addresses these concerns. Overall, our results indicate that the inverse relationship between AROCM and mammalian lifespan persist even after adjusting for these confounders. Future studies could explore whether rates of change in methylation differs between the sexes. Also, it will be intriguing to explore interventions that impact the AROCM. Many interventions influencing the lifespan of mice have been linked to alterations in age-associated methylation [23, 29, 34, 36, 43, 48]. While we present essential equations that connect epigenetic aging rates to maximum lifespan, this mathematical framework also holds significant relevance for numerous other aging biomarkers.

Methods

Methylation Platform

Both dog and mammalian data were generated using the same HorvathMammalMethylChip40 platform, which offers high coverage of approximately 36K conserved CpGs in mammals [2]. To minimize technical variation, all data were generated by a single lab (Horvath) using a single, consistent measurement platform. Preprocessing and normalization were performed using the SeSaMe method to define beta values for each probe [51]. The chip manifest file is available on the Gene Expression Omnibus (GEO) platform GPL28271 and on our Github page [2]).

Chromatin states

Following the pan-mammalian aging study of the Mammalian Methylation Consortium, we grouped the CpGs into 54 universal chromatin states that were covered by at least 5 CpGs each [33]. These 54 chromatin states include those that correspond to constitutive and cell-type-specific activity across diverse human cell and tissue types [47]. For example, we previously found that strong age-related gain of methylation can be observed in bivalent promoter states and other states that are bound by Polycomb group repressive complex 2 (PRC2 binding sites). To facilitate a detailed analysis of PRC2 binding, we split each chromatin state into 2 subsets denoted by "StateName+" or "StateName–" according to PRC2 binding (+ for yes and – for no). In this article we focused on "BivProm2+", which is the set of 552 CpGs that reside in bivalent chromatin state 2 and are bounded by PRC2 (Supplementary Table 5).

Dog methylation data

We analyzed methylation profiles from $n = 742$ blood samples derived from 93 dog breeds (Canis lupus familiaris). Primary characteristics (sex, age, average life expectancy) for the breeds utilized are presented in Supplementary Table 1. Standard breed weight and lifespan were aggregated from several

sources as detailed in [27]. We created consensus values based on the American Kennel Club and the Atlas of Dog Breeds of the World. Lifespan estimates were calculated as the average of the standard breed across sexes, compiled from numerous publications consisting primarily of multibreed surveys of age and cause of death from veterinary clinics and large-scale breed-specific surveys, which are often conducted by purebred dog associations. Sources for median lifespan per dog breed are reported in [27]. We calculated the maximum lifespan per dog breed by multiplying the median lifespan with a factor 1.33, i.e. $MaxLifespan = 1.33 * MedianLifespan$. Our results are qualitatively unchanged if other multipliers are being used. Detailed values on the dog breeds are reported in Supplementary Table 1. Median lifespans of the 93 breeds ranged from 6.3 y (Great Dane, average adult breed weight = 64 kg) to 14.6 y (Toy Poodle, average adult breed weight = 2.3 kg). Median lifespan estimates were based on the combined findings of multiple large-scale breed health publications, utilizing the median and maximum ages for each breed.

Selection of dog strata

We selected strata for which the rate of change in methylation could be robustly estimated. Mathematically speaking, the minimum sample size was $n = 3$. Further, we considered the lower and upper limits of the relative age $\mathbf{R}$, i.e. the age interval $[L, U]$. We excluded strata for the followings reasons.

1. Small sample size $n < 3$.
2. Low standard deviation in relative age, i.e. $\mathrm{SD}(\mathbf{R}) < 0.2$, which excluded two breeds with extreme AROCM values that are > 0.5 (two largest values in all breeds).
3. Bad regression fit of AROCM, i.e. $R^2 < 0.2$, which excluded three smallest AROCM values (two are negative).

Selection of mammalian species/tissue strata

The raw data included 229 species-tissue strata from 126 unique species (Supplementary Figure S14). We selected strata for which the rate of change in methylation could be robustly estimated. Mathematically speaking, the minimum sample size was $n = 3$. Further, we considered the lower and upper limits of the relative age $\mathbf{R}$, i.e. the age interval $[\ell, u]$. We excluded strata for the followings reasons.

1. Small sample size $n < 3$.
2. Low standard deviation in relative age, i.e. $\mathrm{SD}(\mathbf{R}) < 0.06$, to avoid constant age samples.
3. AROCM values out of range (estimate < -1 or > 10) were omitted if the values in derived/adjacent age intervals were not outliers. Toward this end, derived AROCMs were calculated for different age intervals within the same stratum (comprised of species and tissue). For example, a severely outlying value AROCM[0, 0.1*L] was declared an outlier if both $AROCM[0, 0.2 * L]$ and $AROCM[0, 0.3 * L]$ fell within the range $(-1, 10)$ for the same stratum.

Mammalian Methylation Data

When considering the entire age range $[0, Lifespan)$, we analyzed $S = 229$ different species/tissue strata (Supplementary Table 1). Out of the 229 strata, 100 involved blood, 73 skin, 26 brain, and 15 liver strata. Fewer strata were available with the given age range. For example, $S = 128$ for the young age group (defined by $[0, 0.1L]$) and $S = 221$ for the old age group (defined by $[0.1L, L]$). Our data involved 126 different mammalian species. For many species, several tissue types were available. The species characteristics such as maximum lifespan come from an updated version of the anAge data base [15, 22].

Adjusted rate of change and adjusted correlation

In the following, we will present a mathematical formalism that links three measurements: the rate of change in the biomarker across the life course, Pearson correlation between age and the biomarker, and the standard deviation of age. In most data sets, the standard deviation of age is correlated with

maximum lifespan and it reflects the idiosyncracies of the sample collection. The standard deviation of age has a confounding effect on both the rate of change and the correlation between a biomarker (M) and age. To study and to eliminate this confounding effect, we introduce two new concepts: *adjusted* rate of change and *adjusted* Pearson correlation. We present mathematical propositions describing the conditions under which strong relationships between rate of change and lifespan can be observed.

In the following, we derive general equations that link the rate of change (also known as gradient or slope) of any continuous biomarker of aging (denoted as $M \in R$) to the species maximum lifespan. For example, M could denote mean methylation in a particular chromatin state. Assume $\mathbf{M} = (M_1, ..M_n)$ and $\mathbf{A} = (A_1, .., A_n)$ are two numeric vectors of n samples for the biomarker M and the Age variable. We will be using the following definitions surrounding the sample mean, sample variance, sample covariance, and Pearson correlation.

$$\begin{aligned}
\overline{\mathbf{M}} &\doteq \frac{1}{n}\sum_{i=1}^{n} M_i, \\
\mathrm{Var}\,(\mathbf{M}) &\doteq \frac{1}{n}\sum_{i=1}^{n}(M_i - \overline{\mathbf{M}})^2, \\
\mathrm{SD}\,(\mathbf{M}) &\doteq \sqrt{\mathrm{Var}\,(\mathbf{M})} \\
CoefVar(\mathbf{M}) &\doteq \frac{\sqrt{\mathrm{Var}\,(\mathbf{M})}}{\overline{\mathbf{M}}} \\
\mathrm{Cov}(\mathbf{M}, \mathbf{A}) &\doteq \frac{1}{n}\sum_{i=1}^{n}(M_i - \overline{\mathbf{M}})(A_i - \overline{\mathbf{A}}), \\
\mathrm{Cor}(\mathbf{M}, \mathbf{A}) &\doteq \frac{\mathrm{Cov}(\mathbf{M}, \mathbf{A})}{\sqrt{\mathrm{Var}\,(\mathbf{M}) * \mathrm{Var}\,(\mathbf{A})}}.
\end{aligned} \tag{13}$$

Next, we define the rate of change, ROC($\mathbf{M}|\mathbf{A}$), as the change in M resulting from a 1-year increase in age (calendar age in units of years). Statistically speaking, the rate of change, ROC($\mathbf{M}|\mathbf{A}$), is the slope/coefficient β_1 in the univariate linear regression model below,

$$M_i = \beta_0 + \beta_1 A_i + \epsilon_i, \tag{14}$$

where the index i refers to the i-th tissue sample and the expected value of the error term ϵ_i is assumed to be zero. The rate of change can be estimated by the least squares or the maximum likelihood estimator, $\hat{\beta}_1$. Furthermore, it can be expressed in terms of the Pearson correlation coefficient and standard deviations as follows

$$\mathrm{ROC}(\mathbf{M}|\mathbf{A}) \doteq \hat{\beta}_1 = \frac{\mathrm{Cor}(\mathbf{M}, \mathbf{A})\mathrm{SD}\,(\mathbf{M})}{\mathrm{SD}\,(\mathbf{A})}. \tag{15}$$

To arrive at a unit-less biomarker, which lends itself for comparisons with other biomarkers we standardize $\mathbf{M}$ to have mean zero and standard deviation one, by scaling it as below,

$$ScaledM_i \doteq \frac{M_i - \overline{\mathbf{M}}}{\mathrm{SD}\,(\mathbf{M})}. \tag{16}$$

Using SD ($\mathbf{ScaledM}$) = 1, equation (15) becomes

$$\begin{aligned}
\mathrm{ROC}(\mathbf{ScaledM}|\mathbf{A}) \doteq \hat{\beta}_1 &= \frac{\mathrm{Cor}(\mathbf{ScaledM}, \mathbf{A})}{\mathrm{SD}\,(\mathbf{A})} \\
&= \frac{\mathrm{Cor}(\mathbf{M}, \mathbf{A})}{\mathrm{SD}\,(\mathbf{A})}
\end{aligned} \tag{17}$$

where the latter equation used the fact that the Pearson correlation, Cor, is invariant with respect to linear transformations. To reveal the dependence on species maximum lifespan, it is expedient to define relative age as the ratio of age by maximum lifespan:

$$R_i = \frac{A_i}{L}. \tag{18}$$

Since the standard deviation is the square root of the variance, one can easily show that

$$\mathrm{SD}\left(\mathbf{A}\right) = \mathrm{SD}\left(\mathbf{R}\right) * L. \tag{19}$$

Combining equations (17) and (18) results in

$$\mathrm{ROC}(\mathbf{ScaledM}|\mathbf{A}) = \frac{\mathrm{Cor}(\mathbf{M},\mathbf{A})/\mathrm{SD}\left(\mathbf{R}\right)}{L}. \tag{20}$$

Since Pearson's correlation is scale-invariant, the following equality holds and we will use them interchangeably,

$$\mathrm{Cor}(\mathbf{M},\mathbf{A}) = \mathrm{Cor}(\mathbf{ScaledM},\mathbf{A}) = \mathrm{Cor}(\mathbf{M},\mathbf{R}). \tag{21}$$

Proposition 1 (Relationship between ROC and Lifespan)**.** *Assuming*

$$\mathrm{Cor}(\mathbf{M},\mathbf{A})/\mathrm{SD}\left(\mathbf{R}\right) \approx constant \tag{22}$$

equation 20 implies

$$\mathrm{ROC}(\mathbf{ScaledM}|\mathbf{A}) \approx \frac{constant}{L}. \tag{23}$$

In empirical data, the strong assumption 22 is not satisfied, see e.g. Figure S2c. But one can formulate a weaker, more realistic assumption that yields a conclusion similar to that in equation 23. Toward this end, we are rewriting equation (20) by multiplying both sides with the factor $\mathrm{SD}\left(\mathbf{R}\right)^{1-p}$ which depends on the power parameter p:

$$\mathrm{ROC}(\mathbf{ScaledM}|\mathbf{A}) \times \mathrm{SD}\left(\mathbf{R}\right)^{1-p} = \frac{\mathrm{Cor}(\mathbf{M},\mathbf{A})/\mathrm{SD}\left(\mathbf{R}\right)^{p}}{L}. \tag{24}$$

To succinctly express the latter equation, we introduce 2 new definitions:

$$\begin{aligned} Adj.\mathrm{ROC}(\mathbf{ScaledM}|\mathbf{A},p) &\doteq \mathrm{ROC}(\mathbf{ScaledM}|\mathbf{A})\mathrm{SD}\left(\mathbf{R}\right)^{1-p}, \\ Adj.Cor(\mathbf{M}|\mathbf{R},p) &\doteq \frac{\mathrm{Cor}(\mathbf{R},\mathbf{M})}{\mathrm{SD}\left(\mathbf{R}\right)^{p}}. \end{aligned} \tag{25}$$

Note that Adj.ROC becomes the standard definition of the ROC with $p = 1$. On the other hand, $p = 0$ implies that $Adj.Cor(\mathbf{M}|\mathbf{R},p) = \mathrm{Cor}(\mathbf{M},\mathbf{R})$. The novel terminology has several advantages. To begin with, equation 24 can be succinctly written as follows

$$Adj.\mathrm{ROC}(\mathbf{ScaledM}|\mathbf{A},p) = \frac{Adj.Cor(\mathbf{M}|\mathbf{R},p)}{L}. \tag{26}$$

We introduced the novel terminology surrounding the adjusted rate of change and the adjusted correlation since it will allow us state conditions when equation 26 can be simplified as follows

$$Adj.\mathrm{ROC} \approx \frac{constant}{L}. \tag{27}$$

The approximation "≈" is meant to indicate that there is a high linear correlation on the log scale across different species (and tissues). Thus, our starting point is the log transformed version of equation (26):

$$\log(Adj.\mathrm{ROC}(\mathbf{ScaledM}|\mathbf{A},p)) = \log(Adj.Cor(\mathbf{M}|\mathbf{R},p)) - \log(L), \tag{28}$$

where we assume that the natural logarithm (log) is applicable, i.e. the adjusted ROC and the adjusted correlation take on positive values.

The above mentioned definitions and equations apply to each stratum (e.g. a specific dog breed). In the following, we assume that we are dealing with S different strata comprised of different combinations of species and tissue type. To highlight the dependence on the underlying stratum, we introduce a superscript in various quantities e.g. we write $L^{(s)}$, and $Adj.Cor(\mathbf{M}^{(s)}|\mathbf{R}^{(s)},p)$, where $s = 1, 2, .., S$. Define the following 3 vectors that have S components each

$$\begin{aligned} \mathbf{log.L} &= \left(\log(L^{(1)}), \log(L^{(2)}), .., \log(L^{(S)})\right) \\ \mathbf{log.Adj.Cor} &= \left(\log(Adj.Cor(\mathbf{M}^{(s)}|\mathbf{R}^{(s)}))\right)_{1\leq s\leq S} \\ \mathbf{log.Adj.ROC} &= \left(Adj.\mathrm{ROC}(\mathbf{ScaledM}^{(s)}|\mathbf{A}^{(s)}\right)_{1\leq s\leq S}. \end{aligned} \tag{29}$$

For each vector on the left hand side, we can form the sample mean and sample variances across S strata,

$$\overline{\mathbf{log.Adj.Cor}} = \frac{1}{S}\sum_{s=1}^{S}\log(Adj.Cor(\mathbf{M}^{(s)}|\mathbf{R}^{(s)})) \tag{30}$$

$$\mathrm{Var}\left(\mathbf{log.Adj.Cor}\right) = \frac{1}{S}\sum_{s=1}^{S}\left(\log(Adj.Cor(\mathbf{M}^{(s)}|\mathbf{R}^{(s)})) - \overline{\mathbf{log.Adj.Cor}}\right)^2$$

Using these notations, we are now ready to state the following propositions.

Proposition 2 (Correlation between log.Adj.ROC and log.L)**.** *If*

$$\mathrm{Cor}(\mathbf{log.L}, \mathbf{log.Adj.Cor(p)}) = 0 \tag{31}$$

then

$$\mathrm{Cor}(\mathbf{log.L}, \mathbf{log.Adj.ROC(p)}) = \frac{-1}{\sqrt{1 + \mathrm{Var}\left(\mathbf{log.Adj.Cor}\right)/\mathrm{Var}\left(\mathbf{log.L}\right)}} \tag{32}$$

Remark 1 The condition $\mathrm{Cor}(\mathbf{log.L}, \mathbf{log.Adj.Cor(p)}) = 0$ holds when species lifespan and the $Adj.Cor(p)$ are independent across strata. Our methylation data suggest that this condition is approximately satisfied for specific chromatin states.

Remark 2 This proposition suggests that Lifespan and Adj.ROC follow a nearly perfect inverse linear correlation on the log scale (Cor ≈ -1) if $\mathrm{Var}\left(\mathbf{log.Adj.Cor}\right)/\mathrm{Var}\left(\mathbf{log.L}\right) \approx 0$. The latter condition is satisfied for our data from the mammalian methylation consortium.

Proof. Denote vectors $\mathbf{x} = \mathbf{log.L}$ and $\mathbf{y} = \mathbf{log.Adj.ROC}$. With equation (28) we find that the covariance

$$\mathrm{Cov}(\mathbf{x}, \mathbf{y}) = \mathrm{Cov}(\mathbf{log.L}, \mathbf{log.Adj.Cor}) - \mathrm{Cov}(\mathbf{log.L}, \mathbf{log.L})$$

By assumption the first term is zero, which entails that

$$\mathrm{Cov}(\mathbf{x}, \mathbf{y}) = -\mathrm{Cov}\left(\mathbf{log.L}, \mathbf{log.L}\right) = -\mathrm{Var}\left(\mathbf{log.L}\right)$$

Similarly, $\mathrm{Cov}(\mathbf{log.Adj.Cor}, \mathbf{log.L}) = 0$ implies that

$$\begin{aligned}\mathrm{Var}\left(\mathbf{y}\right) &= \mathrm{Var}\left(\mathbf{log.L}\right) - 2 * \mathrm{Cov}(\mathbf{log.L}, \mathbf{log.Adj.Cor}) + \mathrm{Var}\left(\mathbf{log.Adj.Cor}\right) \\ &= \mathrm{Var}\left(\mathbf{log.L}\right) + \mathrm{Var}\left(\mathbf{log.Adj.Cor}\right)\end{aligned}$$

Thus, the assumption implies that

$$\begin{aligned}\mathrm{Cor}(\mathbf{x}, \mathbf{y}) &= \frac{\mathrm{Cov}(x, y)}{\sqrt{\mathrm{Var}\left(x\right)\mathrm{Var}\left(y\right)}} \\ &= -\mathrm{Var}\left(\mathbf{log.L}\right)/\sqrt{\mathrm{Var}\left(\mathbf{log.L}\right) + \mathrm{Var}\left(\mathbf{log.Adj.Cor}\right)} \\ &= -1/\sqrt{1 + \mathrm{Var}\left[\mathbf{log.Adj.Cor}\right]/\mathrm{Var}\left(\mathbf{log.L}\right)},\end{aligned}$$

which concludes one direction of the proof. The other direction of the proof can be similarly deduced. The following proposition is a direct consequence of the proposition.

Proposition 3 (Linear relationship between log.Adj.ROC and log.L)**.** *If for some power p,*

$$Cor(\mathbf{log.L}, \mathbf{log.Adj.Cor(p)}) = 0 \tag{33}$$

and the ratio

$$Ratio(p) = \frac{Var(\mathbf{log.Adj.Cor(p)})}{Var(\mathbf{log.L})} \approx 0, \tag{34}$$

then

$$\mathbf{log.Adj.ROC} \approx \overline{\mathbf{log.Adj.Cor}} - \mathbf{log.L}. \tag{35}$$

Proof. The mean difference between the left hand side, $LHS = log(Adj.ROC^{(s)})$, and the right hand side, $RHS = Mean(log.Adj.Cor) - \log(L^{(s)})$ is zero: $Mean(LHS - RHS) = 0$. Further, theorem 2 coupled with the assumption shows that $Cor(LHS, RHS) \approx 1$ which concludes the proof.

The following proposition applies to most real data sets.

Proposition 4 (Linear relationship between log.Adj.ROC and log.L)**.** *If for some power p,*

$$Cor(\mathbf{log.L}, \mathbf{log.Adj.Cor(p)}) = 0 \tag{36}$$

and the coefficient of variation in $Adj.Cor(p)$ is much smaller than the coefficient of variation in L, i.e.

$$CoefVar(Adj.\mathrm{Cor}(p)) \ll CoefVar(L) \tag{37}$$

then

$$\mathbf{log.Adj.ROC} \approx \overline{\mathbf{log.Adj.Cor}} - \mathbf{log.L}. \tag{38}$$

Proof. In the following, we will show that the assumption (equation 37) implies equation 34 in Proposition 3. Toward this end, we will derive a simple approximation of the variance based on the Delta method for computing the variance of the function $f(X)$ of a random variable X,

$$\mathrm{Var}\left(f(X)\right) \approx f'(\mathrm{E}(X))^2 \mathrm{Var}\left(X\right). \tag{39}$$

where $\mathrm{Var}\left(X\right)$ and $\mathrm{E}(X)$ denote the variance and expectation of X, respectively. With $f(x) = \log(x)$, $f'(x) = 1/x$ and $X = Adj.\mathrm{Cor}(p)$, equation 39 results in

$$\mathrm{Var}\left(\log(Adj.\mathrm{Cor}(p))\right) \approx \frac{\mathrm{Var}\left(Adj.\mathrm{Cor}(p)\right)}{\mathrm{E}(Adj.\mathrm{Cor}(p))^2} = CoefVar^2(Adj.\mathrm{Cor}(p)) \tag{40}$$

where $CoefVar(\cdot)$ denotes the coefficient of variation (equation 13). Analogously, one can show that

$$\mathrm{Var}\left(\log(L)\right) \approx \frac{\mathrm{Var}\left(L\right)}{\mathrm{E}(L)^2} = CoefVar^2(L). \tag{41}$$

This concludes the proof.

After exponentiating both sides of equation 38, we arrive at

$$Adj.\mathrm{ROC}^{(s)} \approx \frac{c(p)}{L^{(s)}} \tag{42}$$

where $c(p) = \exp\left(\overline{\mathbf{log.Adj.Cor}}\right)$. The choice of the parameter p will be discussed in the following.

Criteria for choosing the power p in the adjustment

Our above mentioned equations make use of the parameter p that underlies our definitions of the adjusted correlation and the adjusted ROC. A choice of $p = 1$ results in standard (non-adjusted) versions of the ROC but it can be advantageous to choose a lower value of p for the following three reasons.

First, Proposition 4 states that a strong linear relationship between **log.Adj.ROC** and **L** will result if one choose p such that it minimizes the coefficient of variation function $C(p) = CoefVar(Adj.\mathrm{Cor}(p)$ Since the coefficient of variation is highly sensitive to outliers, we prefer to use a robust version of the coefficient of variation known as the quartile coefficient of dispersion (QCOD):

$$\mathrm{QCOD}(p) \doteq \frac{Q_3(p) - Q_1(p)}{Q_3(p) + Q_1(p)}. \tag{43}$$

where $Q_1(p)$ and $Q_3(p)$ denote the first and third quartile of the distribution of $Adj.\mathrm{Cor}(p)$. In our empirical studies, we chose p so that it minimized QCOD (equation 43), i.e.

$$p_{optimal} = \underset{p}{\mathrm{argmin}}\, \mathrm{QCOD}\left[\log(Adj.\mathrm{Cor}(p))\right] \tag{44}$$

This led to a choice of $p_{optimal} = 0$ for our dog data and $p_{optimal} = 0.25$ for our mammalian methylation data set (Supplementary Figure S1).

The second reason for choosing the power p relates to an undesirable correlation between the age correlation $\mathrm{Cor}(\mathbf{M}, \mathbf{A})$ and the standard deviation of relative age, $\mathrm{SD}(\mathbf{R})$ (Figure S2). Our simulation studies suggests that this positive correlation results from an imperfect sample ascertainment/study design. This can be mitigated against by choosing p so that the *adjusted* age correlation $Adj.\mathrm{Cor}(M|\mathbf{R}, p)$ exhibits a weaker correlation with $\mathrm{SD}(\mathbf{R})$. In the mammalian data, $p = 0.25$ leads to non significant correlation between $Adj.\mathrm{Cor}(M|\mathbf{R}, p)$ and $\mathrm{SD}(\mathbf{R})$ (Figure S2 d, e).

Third, our simulation studies that aimed to emulate our mammalian lifespan data indicate that with large sample sizes per stratum $Adj.\mathrm{Cor}(M|\mathbf{R}, p)$ converges to 1 for $p = 0.25$ (Supplementary Figure (S3). Overall, these results suggest that $p = 0.25$ is a good choice for our mammalian methylation study.

Relation between $AROCM_{young}$ and $AROCM_{old}$

Here, we provide an outline on how to derive a relationship between the rate of change in young animals and that in older ones in the s-th species tissue stratum, i.e.

$$AROCM^{(s)}_{young} = constant * AROCM^{(s)}_{old}. \tag{45}$$

where *constant* denotes a number. We start out with commenting on our definition of relative age. When dealing with prenatal samples (whose chronological ages take negative values), it can be advantageous to slightly modify the definition of relative age as $R = \frac{A+GT}{L+GT}$, by including gestation time (GT) to avoid negative relative ages. For simplicity, we will assume that our data only contains postnatal samples, allowing us to define relative age as $R = \frac{A}{L}$. Empirically, we find that non-linear relationship between $ScaledM$ and relative age in each stratum can be approximated using the following function:

$$\begin{aligned} ScaledM^{(s)}_i &= f(R; \gamma) \\ &= \gamma^{(s)}_0 + \gamma^{(s)}_1 g(R), \end{aligned} \tag{46}$$

where $\gamma^{(s)} = (\gamma^{(s)}_0, \gamma^{(s)}_1)$ are stratum-specific constants. Our empirical studies demonstrate that the following log linear function fits the data quite well.

$$g(R) = \begin{cases} 10R - 1 & R \geq 0.1 \\ \log(10R) & R < 0.1 \end{cases} \tag{47}$$

Note that the first derivative of $g()$ is given by

$$g'(R) = \begin{cases} 10 & R \geq 0.1 \\ 1/R & R < 0.1 \end{cases} \tag{48}$$

Assuming a linear relationship between $ScaledM$ and A and a suitably chosen point A_0, one can approximate AROCM as follows

$$\begin{aligned} AROCM &\approx \frac{\Delta ScaledM}{\Delta A} \\ &\approx \frac{d}{dA}(ScaledM^{(s)})|_{A_0} \\ &= \frac{d}{dA} f(\frac{A}{L})|_{A_0} \\ &= \frac{d}{dR} f(R)|_{R_0} \frac{1}{L} \\ &= \gamma_1 * g'(R_0) \frac{1}{L} \end{aligned} \tag{49}$$

where $R_0 = A_0/L$ and we used the chain rule of calculus. We define the AROCM in young and old animals as the first derivative evaluate at A_{young} and A_{old}, respectively. These ages should be chosen so that the corresponding relative ages R_{young} and R_{old} take on values < 0.1 and > 0.1, respectively. With equations 48 and 49, we find

$$\begin{aligned} AROCM_{young} &= \gamma_1 * \frac{1}{R_{young} L} \\ AROCM_{old} &= \gamma_1 * \frac{10}{L} \end{aligned} \tag{50}$$

With superscripts denoting the s-th species tissue stratum, the latter implies the following linear relationship between the two aging rates

$$AROCM_{young}^{(s)} = \frac{1}{10R_{young}^{(s)}} * AROCM_{old}^{(s)}. \tag{51}$$

If $R_{young}^{(s)}$ is roughly constant then the latter implies that $AROCM_{young}^{(s)} = c*AROCM_{old}^{(s)}$. Empirically, we can verify the latter relationship (Figure 5). Across species-tissue strata, we find that c has a mean value 7.33 and standard deviation 6.8.

Acknowledgements

Competing Interests

SH is a founder of the non-profit Epigenetic Clock Development Foundation which licenses several patents from his former employer UC Regents. The other authors declare no conflicts of interest.

Data Availability

Individual level data from the Mammalian Methylation Consortium will be distributed via Gene Expression Omnibus once the primary citation of the Mammalian Methylation Consortium has been published [22]. The mammalian array platform is distributed by the non-profit Epigenetic Clock Development Foundation (https://clockfoundation.org/). The manifest file of the mammalian array and genome annotations of the CpGs can be found on Github (doi: 10.5281/zenodo.7574747).

Funding

This work was supported by the Paul G. Allen Frontiers Group (SH) and a grant by Open Philanthropy (SH).

Correspondence

Correspondence to Zhe Fei (feiz@g.ucla.edu) and Steve Horvath (shorvath@altoslabs.com)

References

[1] J. Allman, T. McLaughlin, and A. Hakeem. Brain weight and life-span in primate species. *Proceedings of the National Academy of Sciences*, 90(1):118–122, 1993.

[2] A. Arneson, A. Haghani, M. J. Thompson, M. Pellegrini, S. B. Kwon, H. Vu, E. Maciejewski, M. Yao, C. Z. Li, A. T. Lu, et al. A mammalian methylation array for profiling methylation levels at conserved sequences. *Nature communications*, 13(1):1–13, 2022.

[3] S. N. Austad. Diverse aging rates in metazoans: targets for functional genomics. *Mechanisms of ageing and development*, 126(1):43–49, 2005.

[4] M. V. Blagosklonny. Aging is not programmed: genetic pseudo-program is a shadow of developmental growth. *Cell cycle*, 12(24):3736–3742, 2013.

[5] J. J. Boonekamp, G. Mulder, H. M. Salomons, C. Dijkstra, and S. Verhulst. Nestling telomere shortening, but not telomere length, reflects developmental stress and predicts survival in wild birds. *Proceedings of the Royal Society B: Biological Sciences*, 281(1785):20133287, 2014.

[6] A. Cagan, A. Baez-Ortega, N. Brzozowska, F. Abascal, T. H. Coorens, M. A. Sanders, A. R. Lawson, L. M. Harvey, S. Bhosle, D. Jones, et al. Somatic mutation rates scale with lifespan across mammals. *Nature*, 604(7906):517–524, 2022.

[7] W. Calder. Size, function, and life history harvard university press. *Cambridge, Mass*, 1984.

[8] R. M. Cawthon, H. D. Meeks, T. A. Sasani, K. R. Smith, R. A. Kerber, E. O'Brien, L. Baird, M. M. Dixon, A. P. Peiffer, M. F. Leppert, et al. Germline mutation rates in young adults predict longevity and reproductive lifespan. *Scientific reports*, 10(1):10001, 2020.

[9] E. L. Charnov. *Life history invariants: some explorations of symmetry in evolutionary ecology*, volume 6. Oxford University Press, USA, 1993.

[10] R. G. Cutler. Evolution of human longevity: a critical overview. *Mechanisms of Ageing and Development*, 9(3-4):337–354, 1979.

[11] B. Dantzer and Q. E. Fletcher. Telomeres shorten more slowly in slow-aging wild animals than in fast-aging ones. *Experimental gerontology*, 71:38–47, 2015.

[12] J. P. De Magalhães. Species selection in comparative studies of aging and antiaging research. *Handbook of models for human aging*, pages 9–20, 2006.

[13] J. P. de Magalhães. Ageing as a software design flaw. *Genome Biology*, 24(1):1–20, 2023.

[14] J. P. de Magalhães and G. M. Church. Genomes optimize reproduction: aging as a consequence of the developmental program. *Physiology*, 20(4):252–259, 2005.

[15] J. P. De Magalhães, J. Costa, and G. M. Church. An analysis of the relationship between metabolism, developmental schedules, and longevity using phylogenetic independent contrasts. *The Journals of Gerontology Series A: Biological Sciences and Medical Sciences*, 62(2):149–160, 2007.

[16] J. P. De Magalhães, J. Costa, and O. Toussaint. Hagr: the human ageing genomic resources. *Nucleic acids research*, 33(suppl_1):D537–D543, 2005.

[17] C. Farrell, S. Snir, and M. Pellegrini. The epigenetic pacemaker: modeling epigenetic states under an evolutionary framework. *Bioinformatics*, 36(17):4662–4663, 2020.

[18] J. Felsenstein. Phylogenies and the comparative method. *The American Naturalist*, 125(1):1–15, 1985.

[19] C. E. Finch and M. C. Pike. Maximum life span predictions from the gompertz mortality model. *The Journals of Gerontology Series A: Biological Sciences and Medical Sciences*, 51(3):B183–B194, 1996.

[20] D. Gems. The hyperfunction theory: an emerging paradigm for the biology of aging. *Ageing research reviews*, page 101557, 2022.

[21] E. E. Guevara, R. R. Lawler, N. Staes, C. M. White, C. C. Sherwood, J. J. Ely, W. D. Hopkins, and B. J. Bradley. Age-associated epigenetic change in chimpanzees and humans. *Philosophical Transactions of the Royal Society B*, 375(1811):20190616, 2020.

[22] A. Haghani, A. Lu, C. Li, T. Robeck, K. Belov, C. Breeze, R. Brooke, S. Clarke, C. Faulkes, Z. Fei, S. Ferguson, C. Finno, V. Gladyshev, V. Gorbunova, R. Goya, A. Hogan, C. Hogg, T. Hore, H. Kiaris, P. Kordowitzki, G. Banks, W. Koski, K. Mozhui, A. Naderi, E. Ostrander, K. Parsons, J. Plassais, J. Robbins, K. Sears, A. Seluanov, K. Steinman, B. Szladovits, M. Thompson, D. Villar, N. Wang, G. Wilkinson, B. Young, J. Zhang, J. Zoller, J. Ernst, X. Yang, K. Raj, and S. Horvath. Dna methylation networks underlying mammalian traits. *bioRxiv*, 2021.

[23] O. Hahn, S. Grönke, T. M. Stubbs, G. Ficz, O. Hendrich, F. Krueger, S. Andrews, Q. Zhang, M. J. Wakelam, A. Beyer, et al. Dietary restriction protects from age-associated dna methylation and induces epigenetic reprogramming of lipid metabolism. *Genome biology*, 18:1–18, 2017.

[24] P. H. Harvey and M. D. Pagel. *The comparative method in evolutionary biology*, volume 239. Oxford university press Oxford, 1991.

[25] M. F. Haussmann, D. W. Winkler, K. M. O'Reilly, C. E. Huntington, I. C. Nisbet, and C. M. Vleck. Telomeres shorten more slowly in long-lived birds and mammals than in short–lived ones. *Proceedings of the Royal Society of London. Series B: Biological Sciences*, 270(1522):1387–1392, 2003.

[26] S. Horvath. Dna methylation age of human tissues and cell types. *Genome biology*, 14(10):1–20, 2013.

[27] S. Horvath, A. T. Lu, A. Haghani, J. A. Zoller, C. Z. Li, A. R. Lim, R. T. Brooke, K. Raj, A. Serres-Armero, D. L. Dreger, et al. Dna methylation clocks for dogs and humans. *Proceedings of the National Academy of Sciences*, 119(21):e2120887119, 2022.

[28] S. Horvath and K. Raj. Dna methylation-based biomarkers and the epigenetic clock theory of ageing. *Nature Reviews Genetics*, 19(6):371–384, 2018.

[29] C. Kerepesi, B. Zhang, S.-G. Lee, A. Trapp, and V. N. Gladyshev. Epigenetic clocks reveal a rejuvenation event during embryogenesis followed by aging. *Science advances*, 7(26):eabg6082, 2021.

[30] T. B. Kirkwood and S. N. Austad. Why do we age? *Nature*, 408(6809):233–238, 2000.

[31] S. Kumar, G. Stecher, M. Suleski, and S. B. Hedges. Timetree: a resource for timelines, timetrees, and divergence times. *Molecular biology and evolution*, 34(7):1812–1819, 2017.

[32] R. Lowe, C. Barton, C. A. Jenkins, C. Ernst, O. Forman, D. S. Fernandez-Twinn, C. Bock, S. J. Rossiter, C. G. Faulkes, S. E. Ozanne, et al. Ageing-associated dna methylation dynamics are a molecular readout of lifespan variation among mammalian species. *Genome biology*, 19(1):1–8, 2018.

[33] A. T. Lu, Z. Fei, A. Haghani, T. R. Robeck, J. A. Zoller, C. Z. Li, J. Zhang, J. Ablaeva, D. M. Adams, J. Almunia, et al. Universal dna methylation age across mammalian tissues. *BioRxiv*, 2021.

[34] S. Maegawa, Y. Lu, T. Tahara, J. T. Lee, J. Madzo, S. Liang, J. Jelinek, R. J. Colman, and J.-P. J. Issa. Caloric restriction delays age-related methylation drift. *Nature communications*, 8(1):539, 2017.

[35] B. Milholland, X. Dong, L. Zhang, X. Hao, Y. Suh, and J. Vijg. Differences between germline and somatic mutation rates in humans and mice. *Nature communications*, 8(1):15183, 2017.

[36] D. A. Petkovich, D. I. Podolskiy, A. V. Lobanov, S.-G. Lee, R. A. Miller, and V. N. Gladyshev. Using dna methylation profiling to evaluate biological age and longevity interventions. *Cell metabolism*, 25(4):954–960, 2017.

[37] D. E. Promislow. On size and survival: progress and pitfalls in the allometry of life span. *Journal of gerontology*, 48(4):B115–B123, 1993.

[38] V. K. Rakyan, T. A. Down, S. Maslau, T. Andrew, T.-P. Yang, H. Beyan, P. Whittaker, O. T. McCann, S. Finer, A. M. Valdes, et al. Human aging-associated dna hypermethylation occurs preferentially at bivalent chromatin domains. *Genome research*, 20(4):434–439, 2010.

[39] K. Schmidt-Nielsen and S.-N. Knut. *Scaling: why is animal size so important?* Cambridge university press, 1984.

[40] A. Seluanov, V. N. Gladyshev, J. Vijg, and V. Gorbunova. Mechanisms of cancer resistance in long-lived mammals. *Nature Reviews Cancer*, 18(7):433–441, 2018.

[41] J. R. Speakman. Body size, energy metabolism and lifespan. *Journal of Experimental Biology*, 208(9):1717–1730, 2005.

[42] S. C. Stearns. Life history evolution: successes, limitations, and prospects. *Naturwissenschaften*, 87(11):476–486, 2000.

[43] T. M. Stubbs, M. J. Bonder, A.-K. Stark, F. Krueger, F. von Meyenn, O. Stegle, and W. Reik. Multi-tissue dna methylation age predictor in mouse. *Genome biology*, 18(1):1–14, 2017.

[44] X. Tian, A. Seluanov, and V. Gorbunova. Molecular mechanisms determining lifespan in short-and long-lived species. *Trends in Endocrinology & Metabolism*, 28(10):722–734, 2017.

[45] G. M. Tricola, M. J. Simons, E. Atema, R. K. Boughton, J. Brown, D. C. Dearborn, G. Divoky, J. A. Eimes, C. E. Huntington, A. S. Kitaysky, et al. The rate of telomere loss is related to maximum lifespan in birds. *Philosophical Transactions of the Royal Society B: Biological Sciences*, 373(1741):20160445, 2018.

[46] E. Vera, B. B. de Jesus, M. Foronda, J. M. Flores, and M. A. Blasco. The rate of increase of short telomeres predicts longevity in mammals. *Cell reports*, 2(4):732–737, 2012.

[47] H. Vu and J. Ernst. Universal annotation of the human genome through integration of over a thousand epigenomic datasets. *Genome biology*, 23(1):1–37, 2022.

[48] T. Wang, B. Tsui, J. F. Kreisberg, N. A. Robertson, A. M. Gross, M. K. Yu, H. Carter, H. M. Brown-Borg, P. D. Adams, and T. Ideker. Epigenetic aging signatures in mice livers are slowed by dwarfism, calorie restriction and rapamycin treatment. *Genome biology*, 18:1–11, 2017.

[49] K. Whittemore, E. Vera, E. Martínez-Nevado, C. Sanpera, and M. A. Blasco. Telomere shortening rate predicts species life span. *Proceedings of the National Academy of Sciences*, 116(30):15122–15127, 2019.

[50] G. S. Wilkinson, D. M. Adams, A. Haghani, A. T. Lu, J. Zoller, C. E. Breeze, B. D. Arnold, H. C. Ball, G. G. Carter, L. N. Cooper, et al. Dna methylation predicts age and provides insight into exceptional longevity of bats. *Nature communications*, 12(1):1–13, 2021.

[51] W. Zhou, T. J. Triche Jr, P. W. Laird, and H. Shen. Sesame: reducing artifactual detection of dna methylation by infinium beadchips in genomic deletions. *Nucleic acids research*, 46(20):e123–e123, 2018.

Tables and Figures

Table 1: Regression models involving maximum lifespan. We considered animals across the entire age range. We used mean methylation in BivProm2+ for all species-tissue strata ($N = 229$).

Model	Covariate	Estimate	Std. Error	t value	Pr($>|t|$)
M1: $\log(Lifespan) \sim$	(Intercept)	1.54	0.071	21.7	5.40E-52
	log(AROCM)	-0.44	0.026	-16.92	1.80E-35
	log(AverageWeight)	0.09	0.01	9.23	5.10E-18
M2: $\log(AROCM) \sim$	(Intercept)	1.92	0.18	10.94	9.80E-17
	log(Lifespan)	-1.3	0.077	-16.92	1.80E-35
	log(AverageWeight)	0.015	0.02	0.76	0.45
M3: $\log(AROCM) \sim$	(Intercept)	1.7	0.19	9	1.20E-16
	log(Lifespan)	-1.2	0.079	-15	1.80E-35
	log(AverageWeight)	0.015	0.02	0.78	0.43
	Brain	-0.26	0.19	-1.4	0.16
M4: $\log(AROCM) \sim$	(Intercept)	1.79	0.22	8.24	1.94e-14
	log(Lifespan)	-1.28	0.08	-16.06	2e-16
	log(AverageWeight)	0.03	0.02	1.22	0.23
	Brain	0.03	0.21	0.16	0.87
	Blood	0.16	0.15	1.02	0.31
	Skin	0.11	0.16	0.71	0.48
	Liver	0.50	0.23	2.13	0.03
	Muscle	-0.52	0.37	-1.42	0.16
	Tail	0.19	0.33	0.59	0.56

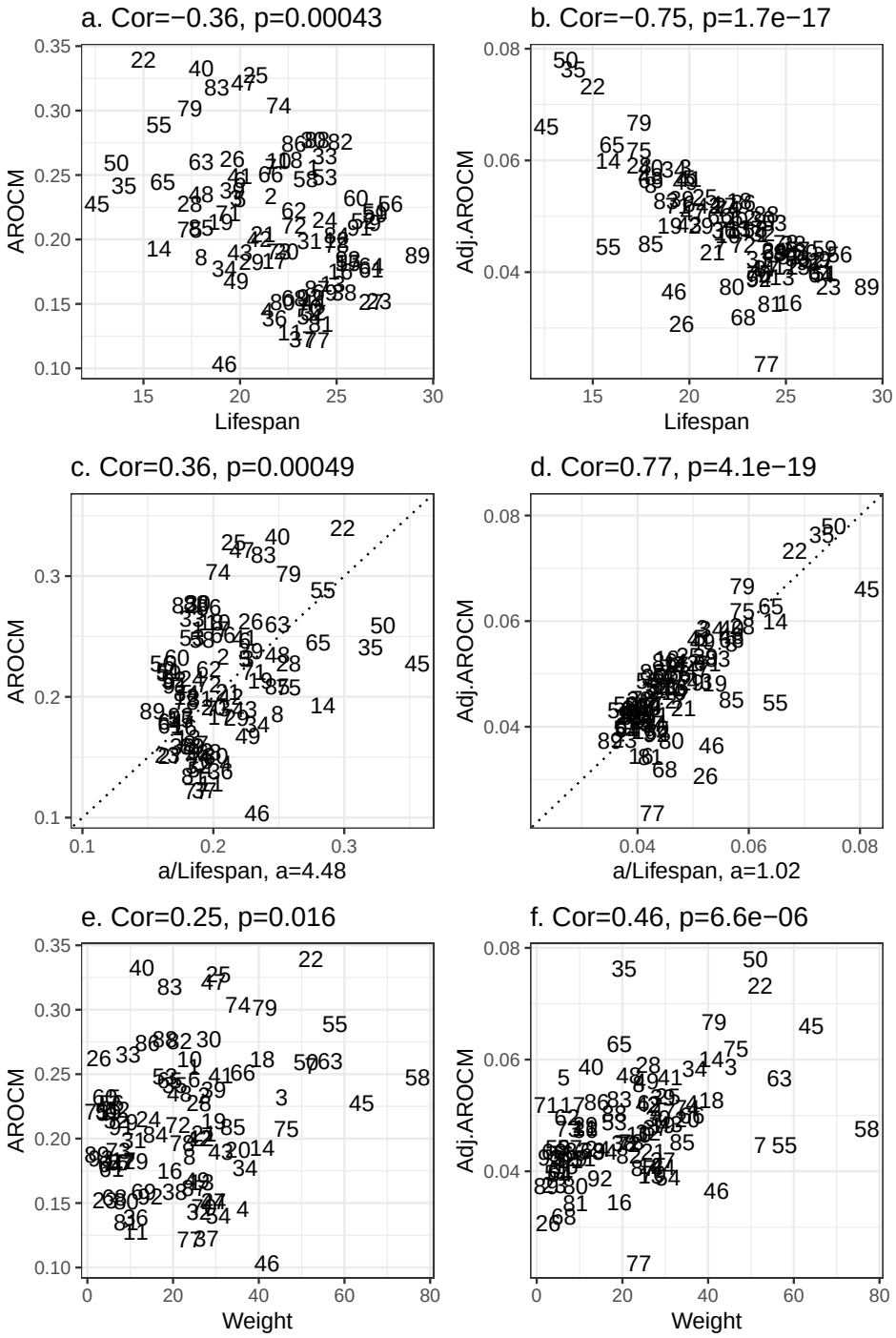

Figure 1: **AROCMs in blood samples from $n = 90$ dog breeds**. Left panels connect AROCMs to Lifespan **(a)**, $a/Lifespan$ **(c)**, and adult weight **(e)**; right panels tie $Adj.AROCM$ to the same factors **(b,d,f)**. Both adjusted and unadjusted AROCMs were computed with $p = 552$ CpGs in bivalent promoter 2 bound by polycomb repressive complex 2 (PRC2) (BivProm2+)[47]. Each integer label corresponds to a different dog breed (Supplementary Table 1).

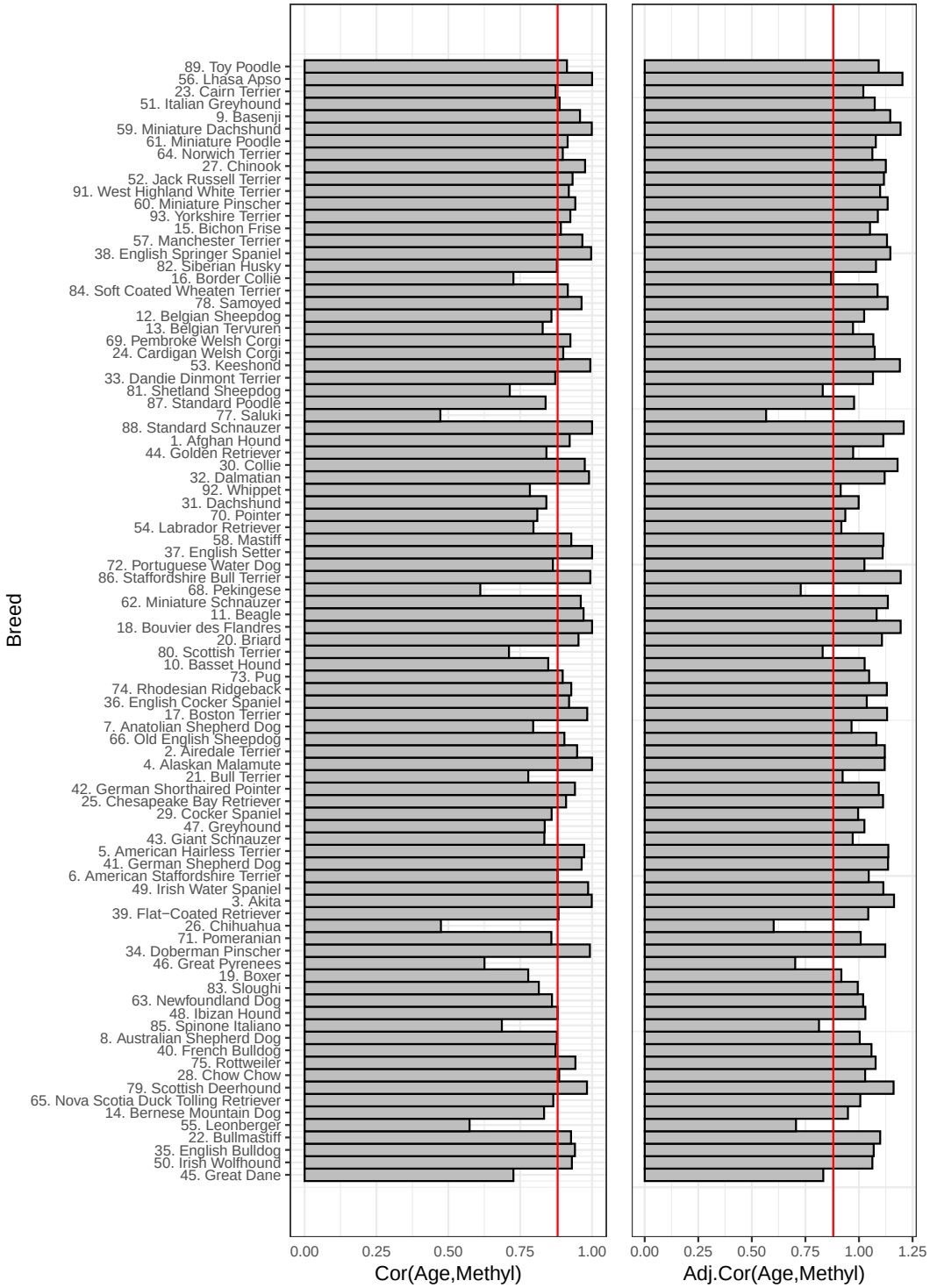

Figure 2: **Cor(Age, Methyl) and Adj.Cor for dog breeds sorted by lifespan.** The correlation between Cor(Age, Methyl) and dog breed lifespans is $0.12(p = 0.25)$; the correlation between Adj.Cor and dog breed lifespans is $0.26(p = 0.01)$. The adjustment power is $p = 0.1$ for Adj.Cor in equation 7.

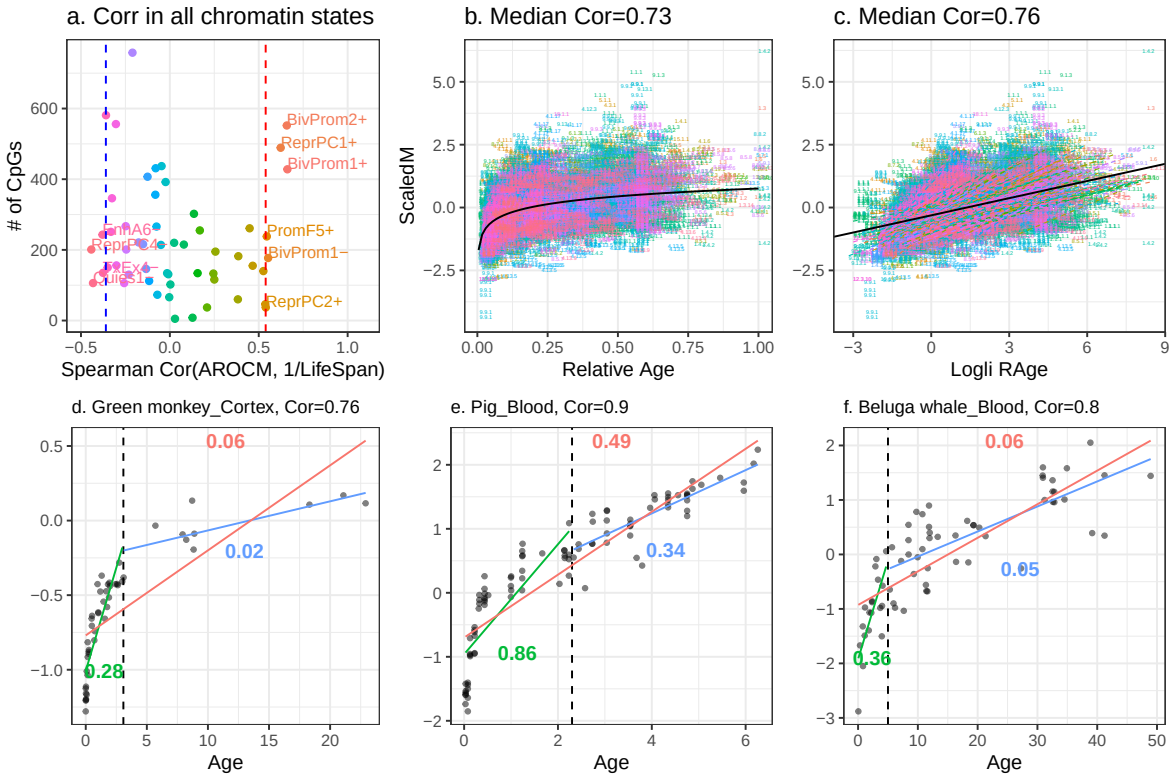

Figure 3: **Age versus mean methylation in select chromatin states in mammals.** **(a)** Displays the Spearman correlation between the inverse of mammalian maximum lifespan $1/L$ (x-axis) and the AROCM of diverse chromatin states. Each dot represents one of the 54 universal chromatin states [47], with the AROCM defined per Methods. Only chromatin states with Spearman correlation exceeding 0.6 or below -0.3 with the inverse of maximum lifespan are labeled. More details are in Supplementary Table 2. The most pronounced correlation is found for CpGs in bivalent promoter 2 also bound by polycomb repressive complex 2 (BivProm2+). **(b)** Scaled Mean Methylation versus Relative Age across all samples; **(c)** Scaled Mean Methylation against Log-linear Transformed Relative Age in all samples. Black curves mark the overall trend. In panel **(c)**, a linear regression line was fitted per species. **(d-f)** Depicts AROCM calculation for BivProm2+ state in 3 species-tissue strata. Colored line segments/numbers in each panel represent: Young AROCM for age interval $[0, 0.1L)$ in green; Old AROCM for age interval $(0.1L, L)$ in blue; AROCM for age interval $[0, L)$ in red.

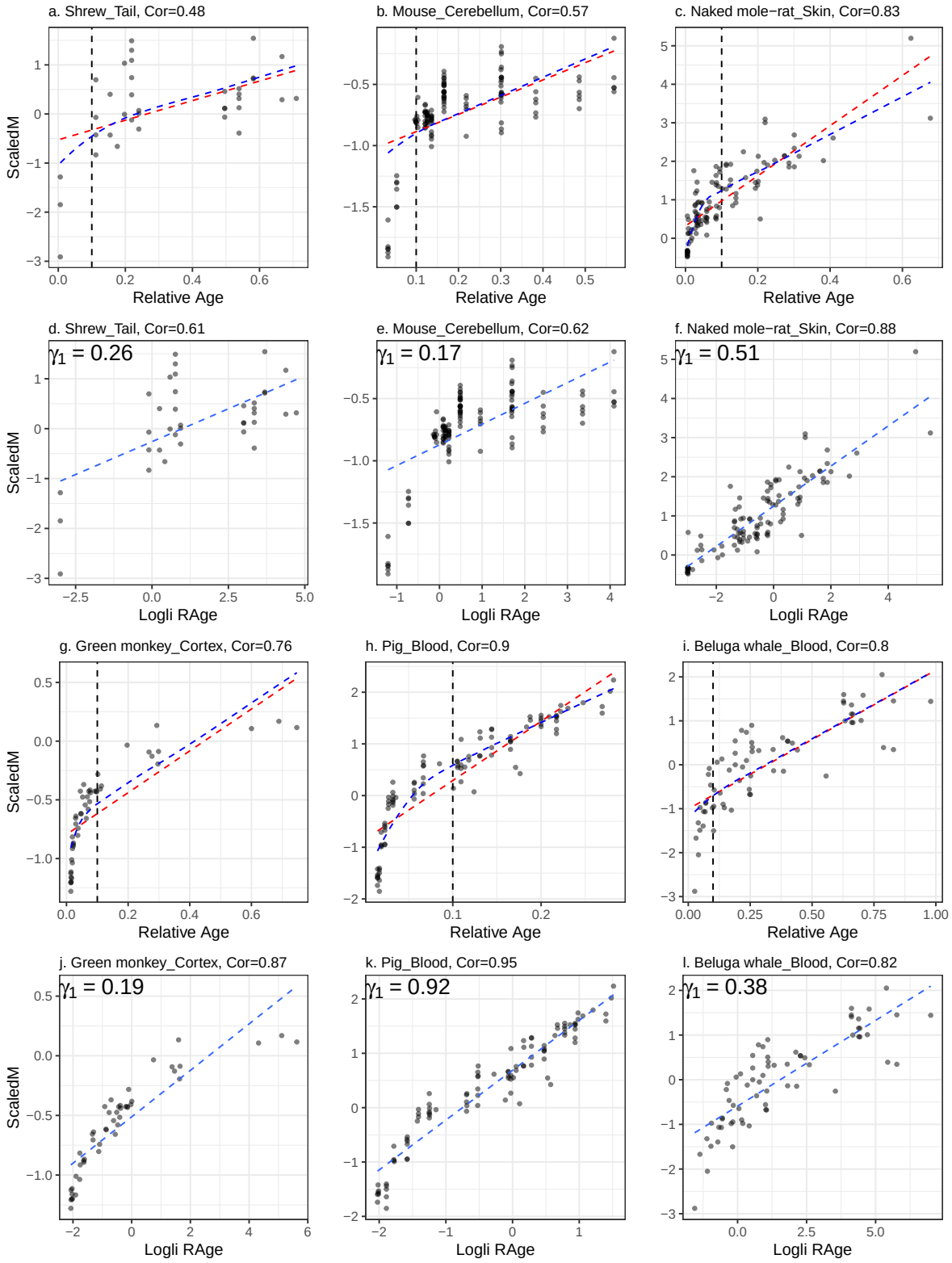

Figure 4: **Scaled Mean Methylation against Relative Age or Loglinear Transformed Relative Age in 6 Additional Species Tissue Strata.** The correlations increase and associations become more linear post transformation. **(a-c, g-i)** Scaled Mean Methylation versus Relative Age, red dashed line represents linear fit to relative age, blue dashed curve represents the inverse transformation of the linear fit in (d-f, j-l); **(d-f, j-l)** Scaled Mean Methylation versus Loglinear transformed relative age, where γ_1 is the AROCM defined in equation 46, with $ScaledM_i = \gamma_0 + \gamma_1 T_i$.

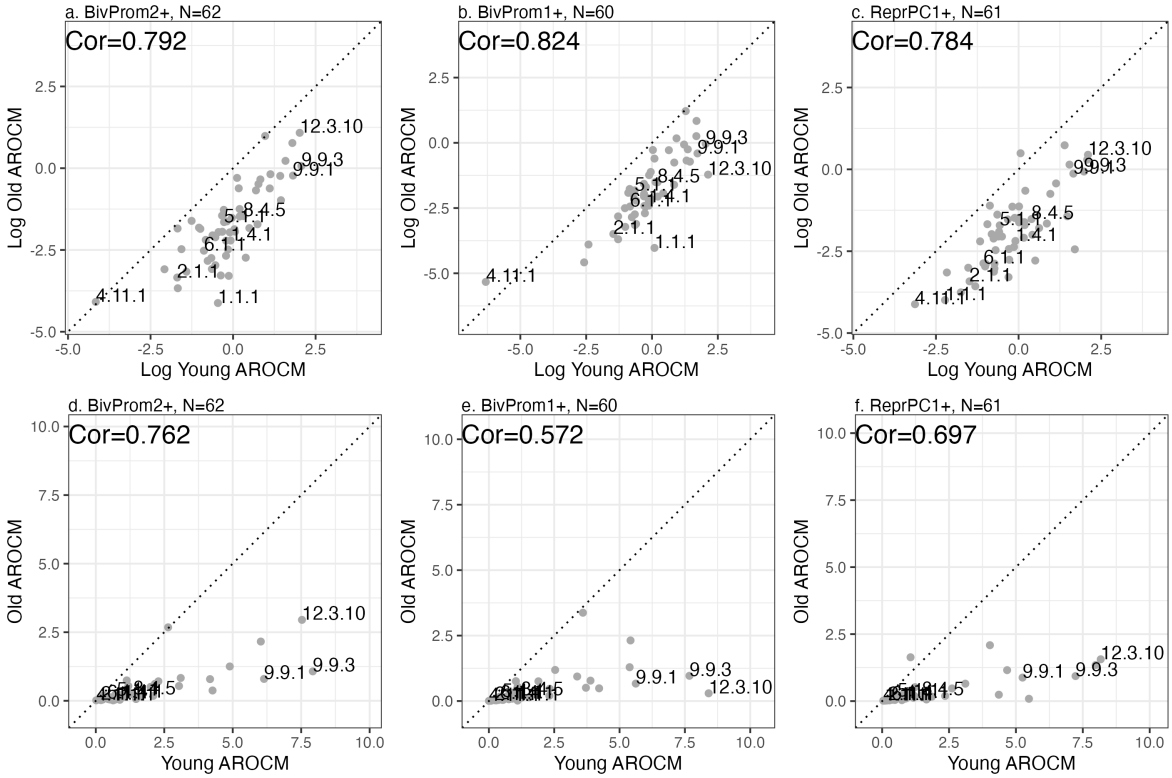

Figure 5: **AROCM in young animals versus that in old animals. (a,b,c)** Natural log transformed values of AROCM in young animals versus AROCM calculated in old animals. Mean methylation was defined with respect to CpGs located in chromatin state **(a)** BivProm2+, **(b)** BivProm1+, **(c)** ReprPC1+. **(d,e,f)** Corresponding plots on the original scale, i.e. without log transformation. Each dot corresponds to a different species. Median aggregation was used to combine AROCM results from different tissues by species. X-axis: AROCM for young samples (Relative Age $R < 0.1$). Y-axis: AROCM for old samples ($R >= 0.1$). Samples are labelled by mammalian species numbers. Each panel reports the Pearson correlation value Cor.

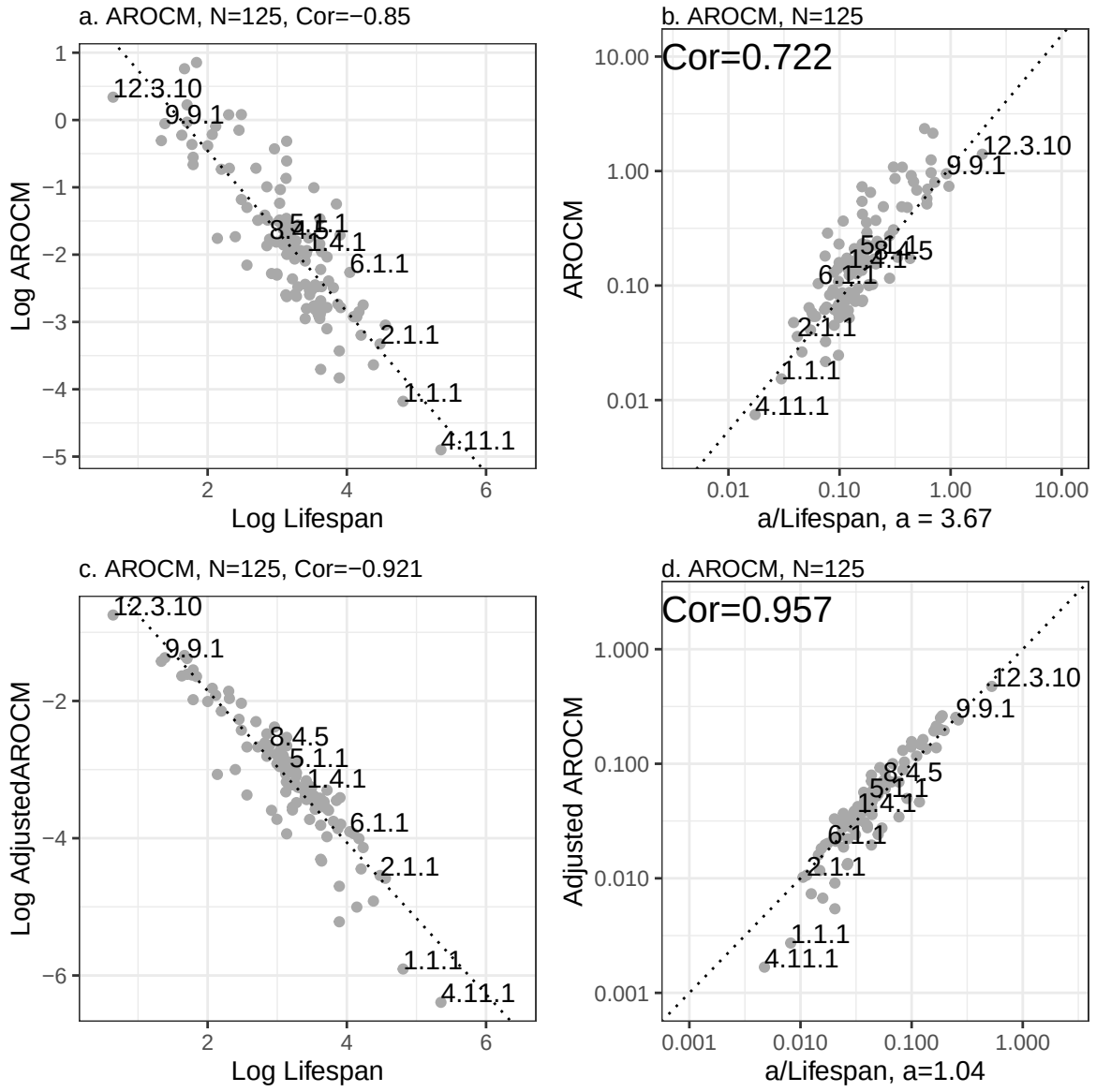

Figure 6: **AROCM Relationship with Maximum Mammalian Lifespan.** **(a)** Log AROCM versus Log Lifespan; **(b)** AROCM against $a/Lifespan$; **(c)** Log Adj.AROCM versus Log Lifespan (equation 28); **(d)** Adj.AROCM against $a/Lifespan$ (equation 42). Figures represent species-level results (median across tissues) with 125 species. Pearson correlations are reported for each panel. Dotted lines in **(b,d)** denote $x = y$. Supplementary Figure S6 contains results for young and old AROCM.

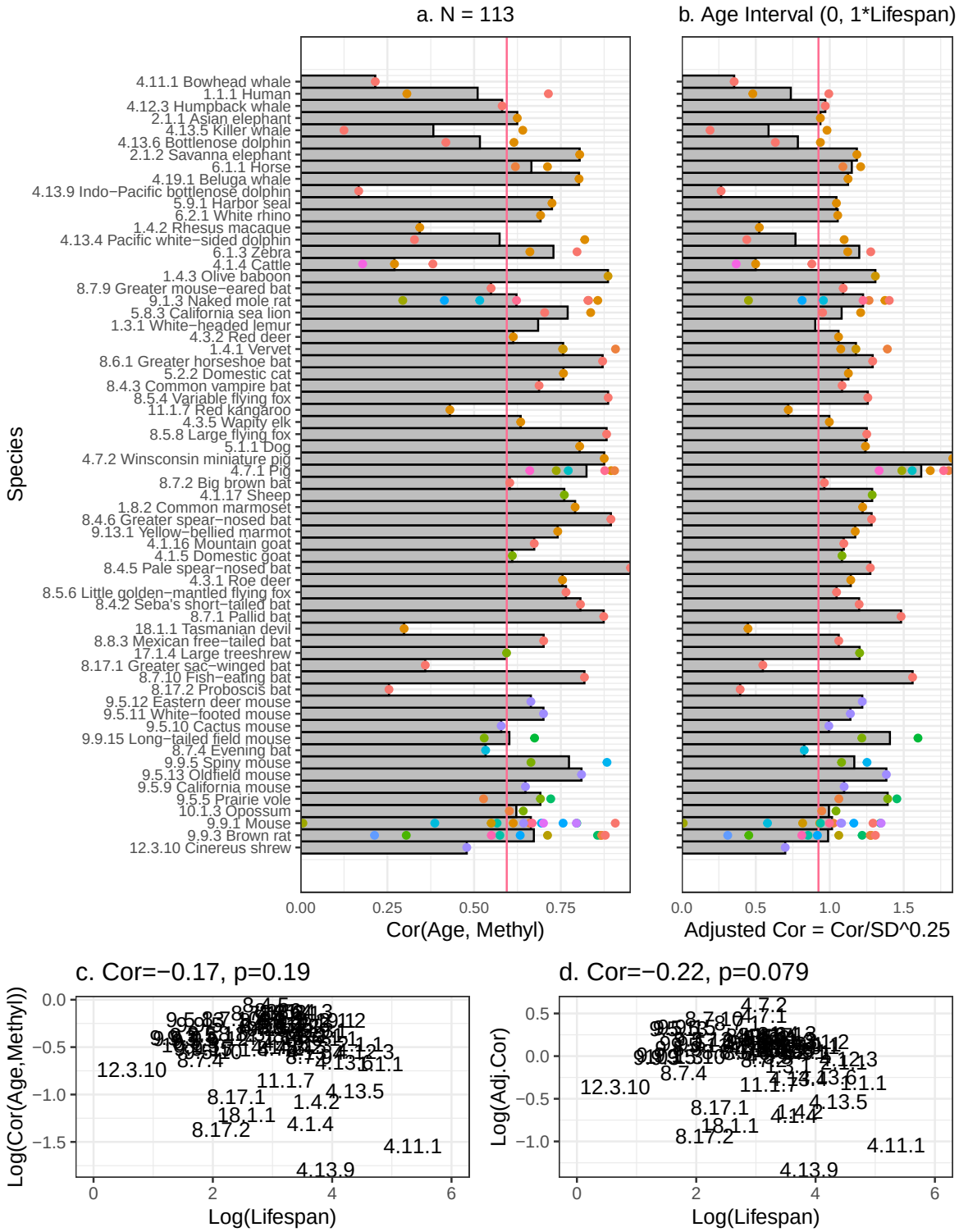

Figure 7: **Species level analysis shows that age correlations do not relate to maximum lifespan (continued to next page).**

Figure 7: Barplot for $Cor(Age, Methyl)$ and $Adj.Cor = \frac{Cor(Age,Methyl)}{\text{SD}(\mathbf{R})^{0.25}}$ (equation 25) in different species (113 species tissue strata with at least 15 samples). Each horizontal bar (y-axis) corresponds to a different species. Species are sorted by maximum lifespan: from long lived (top) to short lived (bottom). The bar length reports the mean value across tissue types of the respective species, while the dots report the values for different tissue types. The QCOD for $Cor(Age, Methyl)$ is 0.189 and that for $Adj.Cor$ is 0.137. Mean and Median $Cor(Age, Methyl)$ across species are 0.66 and 0.69 respectively, and those for $Adj.Cor$ are 1.04 and 1.12. Following equation (1), Methyl was defined as mean methylation value across all CpGs located in bivalent promoter state 2 (BivProm2+). The correlation defined in (33) is **c.** $-0.166(p = 0.19)$ for $Cor(Age, Methyl)$ and **d.** $-0.22(p = 0.08)$ for $Adj.Cor$.

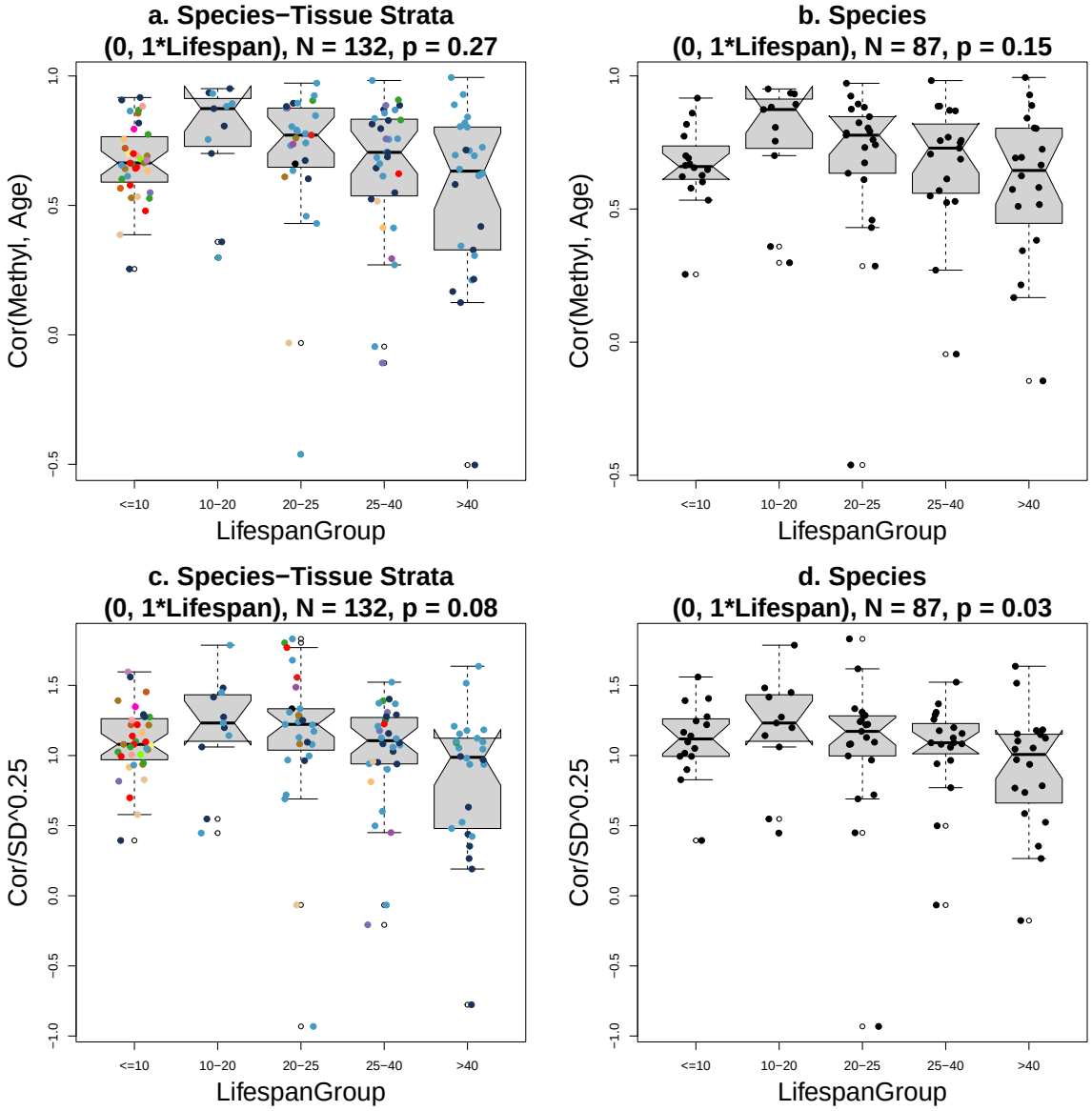

Figure 8: **Lifespan group analysis of age correlations** Cor(Methyl, Age) and $Adj.Cor = \frac{Cor(Methyl,Age)}{SD^{0.25}}$ versus groups of species defined by maximum lifespan. **(a, b)** Non-significant associations between $Cor(Methyl, RelAge)$ and lifespan groups. **(c, d)**: Adjusted Cor (equation 25) by Lifespan groups. P-values are based on the Mann-Kendall Trend Test. These results show that assumption 33 in Proposition 3 is satisfied.

Supplementary Figures

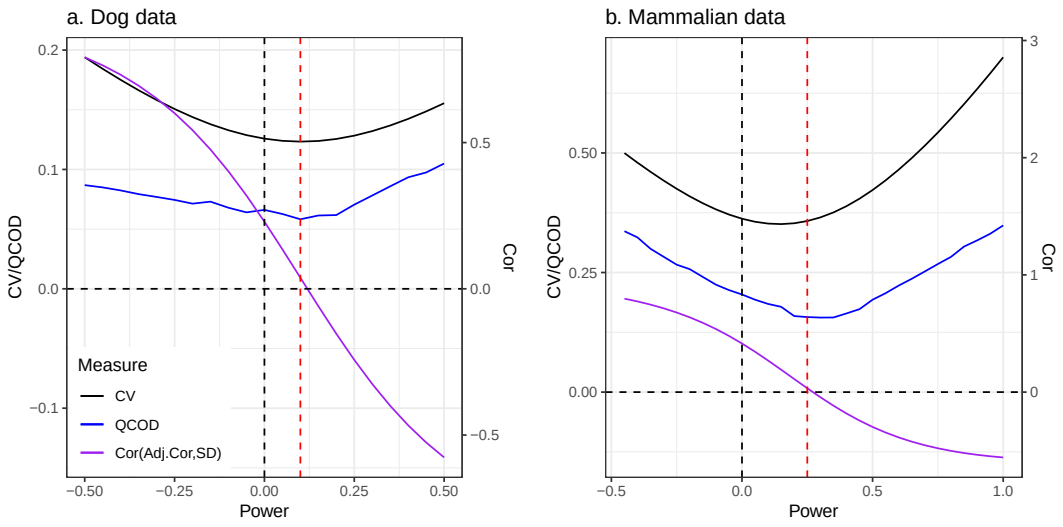

Figure S1: **Choose optimal power for Adj.ROC in (a) Dog data and (b) Mammalian data.** CoefVar (Coefficient of Variation), QCOD, and $\mathrm{Cor}(Adj.\mathrm{Cor}, \mathrm{SD}\,(R))$ are plotted versus different powers. The optimal power (red line) is chosen to be 0.1 for the dog data and 0.25 for the mammalian data.

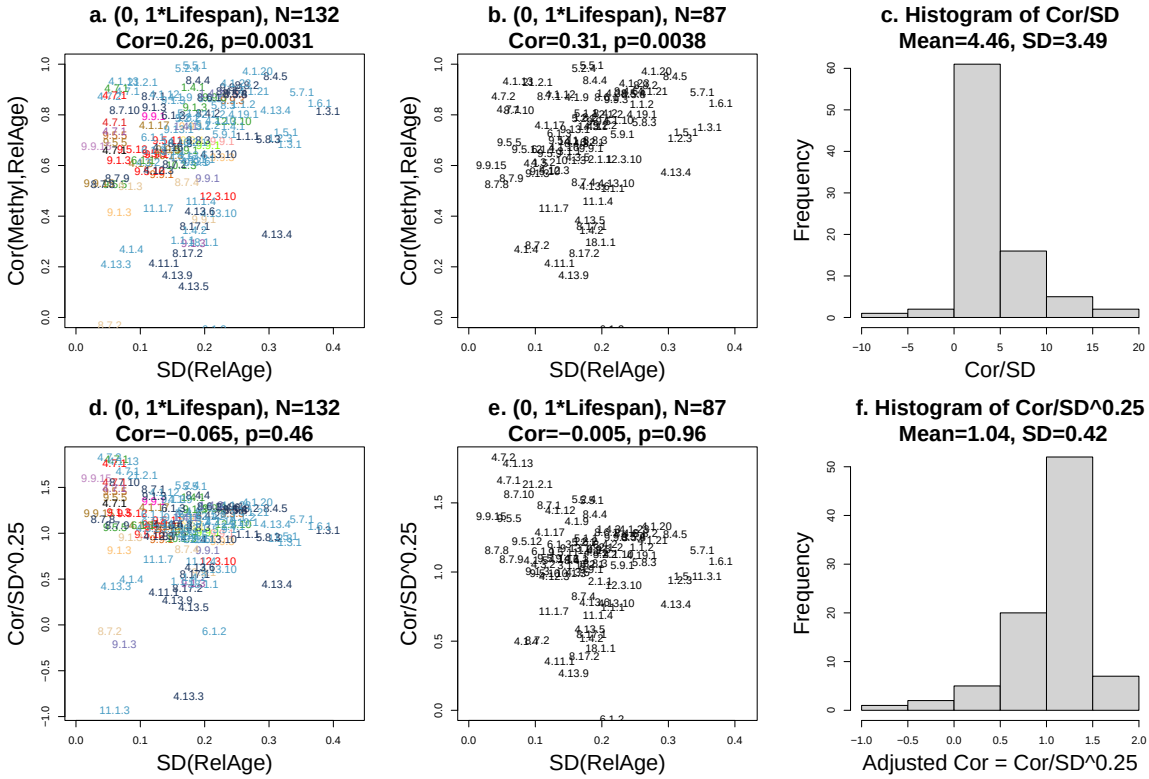

Figure S2: **Age Correlation versus Standard Deviation of Relative Age.** **(a,b)** Show the age correlation $\mathrm{Cor}(M, A)$ and **(d,e)** the adjusted age correlation $Adj.Cor$ against the standard deviation of relative age $\mathrm{SD}(\mathbf{R})$. Age correlation is defined as the Pearson correlation between Mean Methyl (with respect to BivProm2+) and Relative Age for each species-tissue stratum **(a)**, and the species median **(b)**. **(d,e)** Show corresponding results for the adjusted age correlation, using power $p = 0.25$ in equation 25, i.e. $Adj.Cor = \frac{\mathrm{Cor}}{\mathrm{SD}^{0.25}}$. Histograms of **(c)** Cor/SD and **(f)** $Adj.Cor = \mathrm{Cor}/\mathrm{SD}^{0.25}$ are also provided. Titles of scatter plots report Pearson correlation coefficients and associated Student T test p-values. Insignificant Pearson correlation test p values in panels **(d,e)** suggest adjusted age correlations do not correlate with $\mathrm{SD}(R)$, indicating adjusted correlation coefficients provide better resilience against sample ascertainment biases.

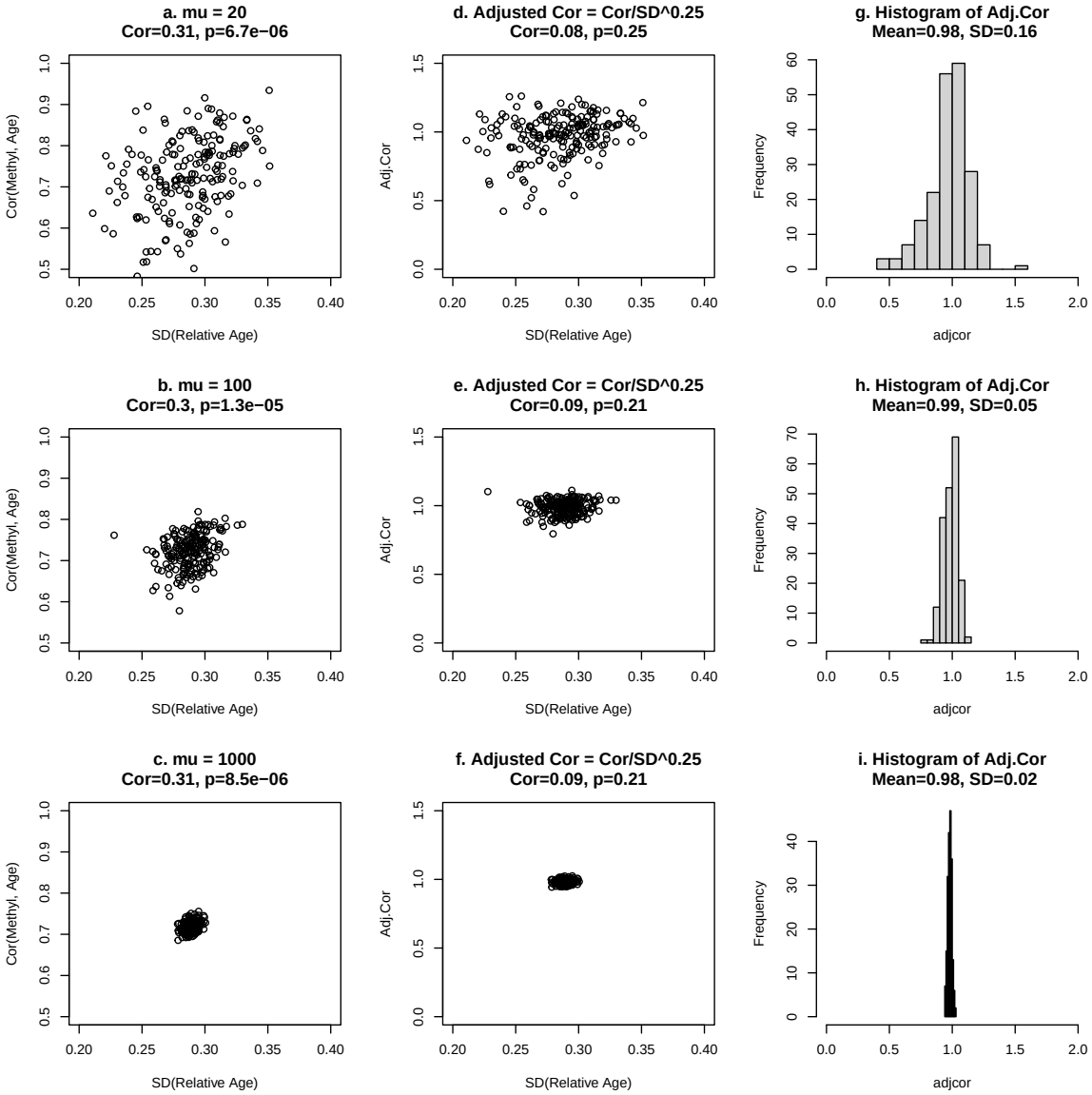

Figure S3: **Simulation Studies: Rationale for Adjusted Correlation Definition.** Panels (a,b,c) show Age correlation cor(M,A) (y-axis) against the standard deviation of relative age (x-axis), revealing a positive Pearson correlation ($Cor \approx 0.3$) due to stratum size variation. Panels (d,e,f) depict Adjusted age correlation (y-axis) against the standard deviation of relative age (x-axis), where the diminished, non-significant Pearson correlation ($Cor \approx 0.09$) demonstrates robustness against variable animal counts. Panels (g,h,i) show histograms of adjusted age correlations, indicating the adjusted correlation's mean value is near 1, and its standard deviation decreases with sample size. These results suggest *Adj.Cor* approaches 1 as stratum size increases. Supplementary Methods provide additional details.

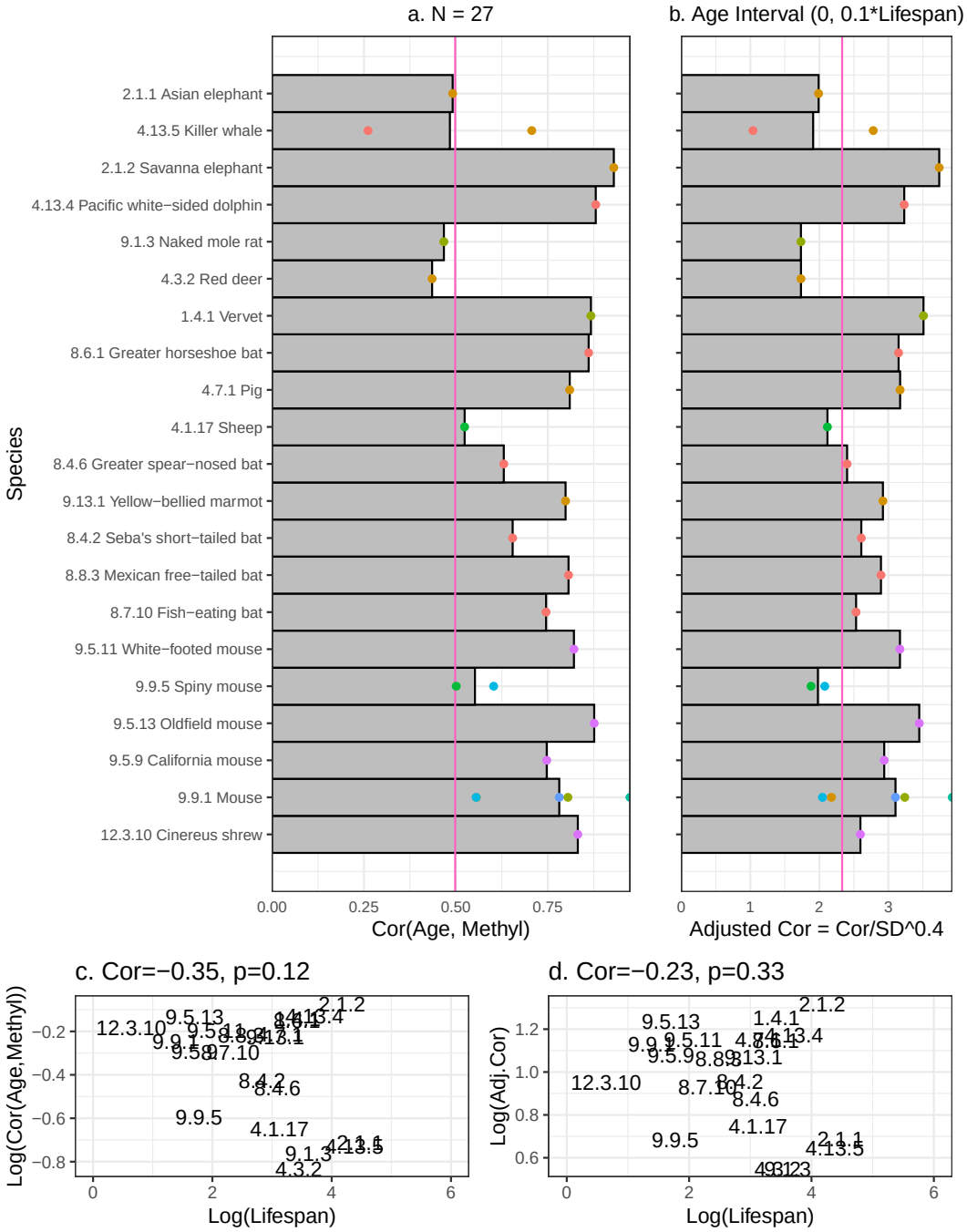

Figure S4: **Species level age correlations in young animals**. This analysis, akin to Figure 7, focuses on younger animals with relative age $R < 0.1$, and species are arranged by lifespan. Each dot represents a different tissue. Panel (a) displays Cor(Age, Mean Methylation in BivProm2+) for strata with sample size >= 15; panel (b) shows Adj.Cor for the same strata. The Mean, Median, and QCOD for Cor(Age,Methyl) are 0.5, 0.6, and 0.137 respectively; for Adj.Cor, they are 2.3, 2.6, and 0.115.

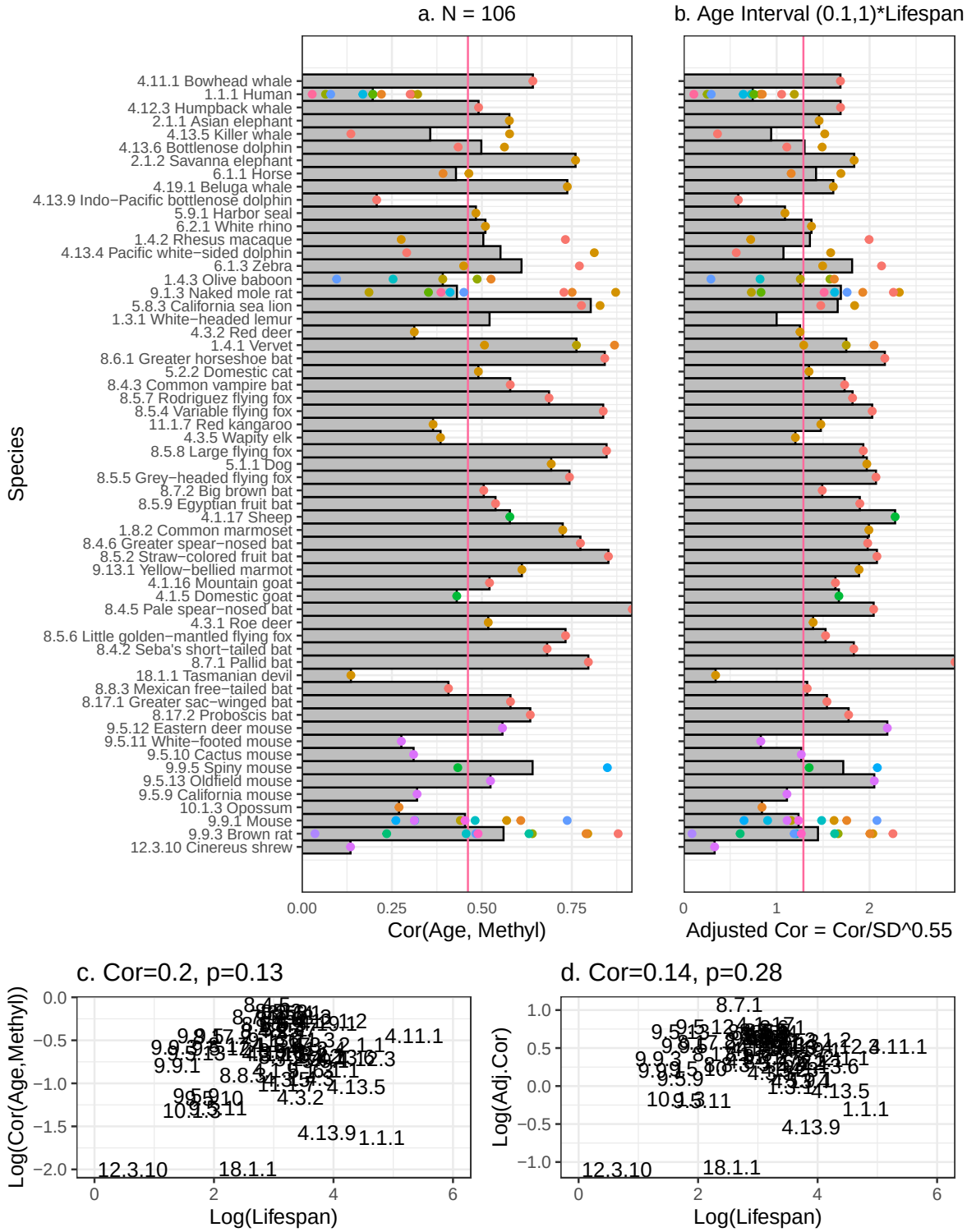

Figure S5: **Species level age correlations in old animals**. This analysis mirrors Figure 7, focusing on older animals with relative age $R \geq 0.1$, and species are sorted by lifespan. Each dot signifies a different tissue. The left panel shows Cor(Age, Mean Methylation) in BivProm2+ for strata with sample size >= 15; the right panel shows Adj.Cor for the same strata. The Mean, Median, and QCOD for Cor(Age,Methyl) are 0.46, 0.51, and 0.389 respectively, and for Adj.Cor, they are 1.17, 1.39, and 0.253.

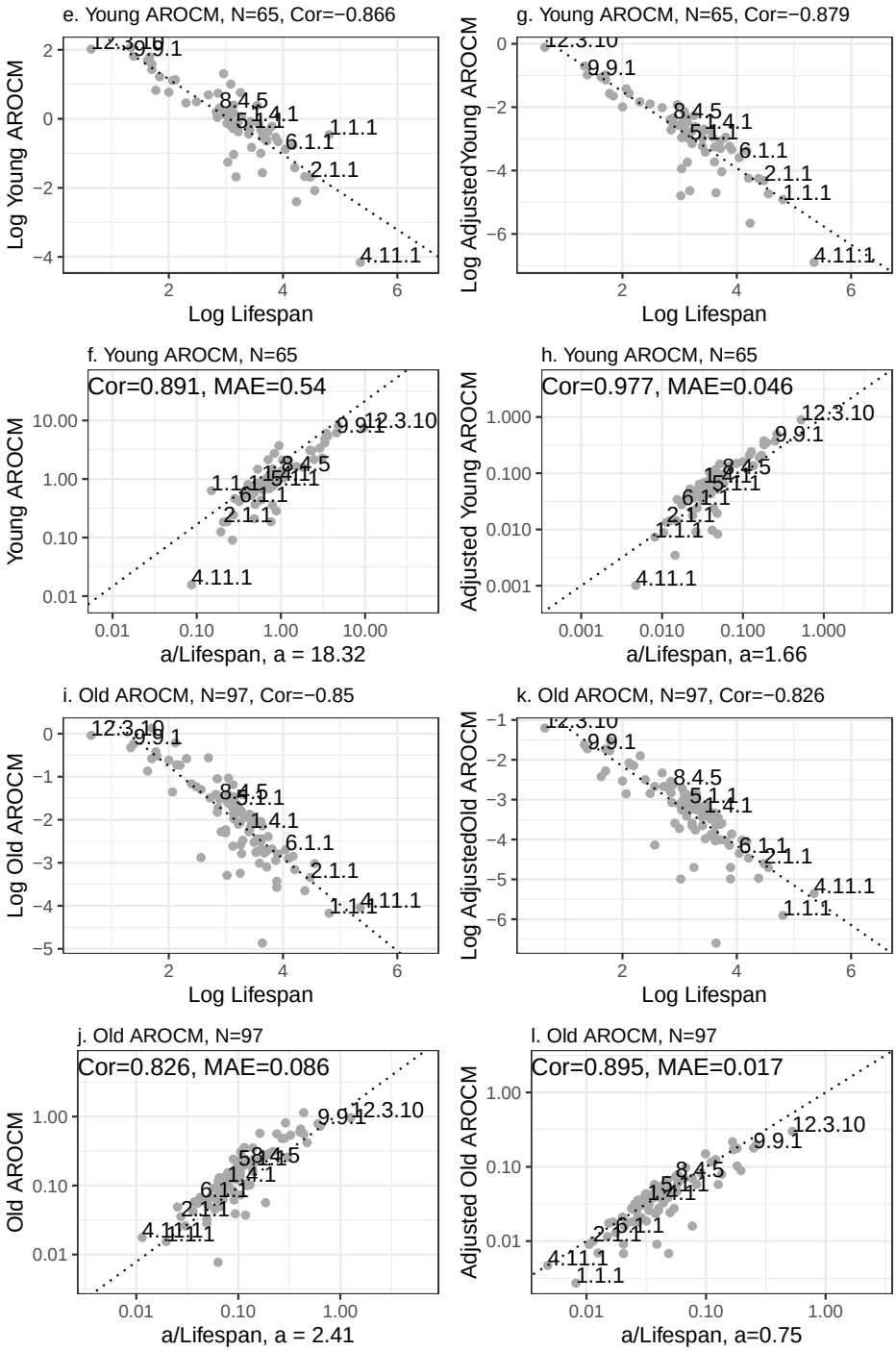

Figure S6: **Young and Old AROCM versus max lifespan.** This figure is analogous to Figure 6 but with Young and Old AROCM.

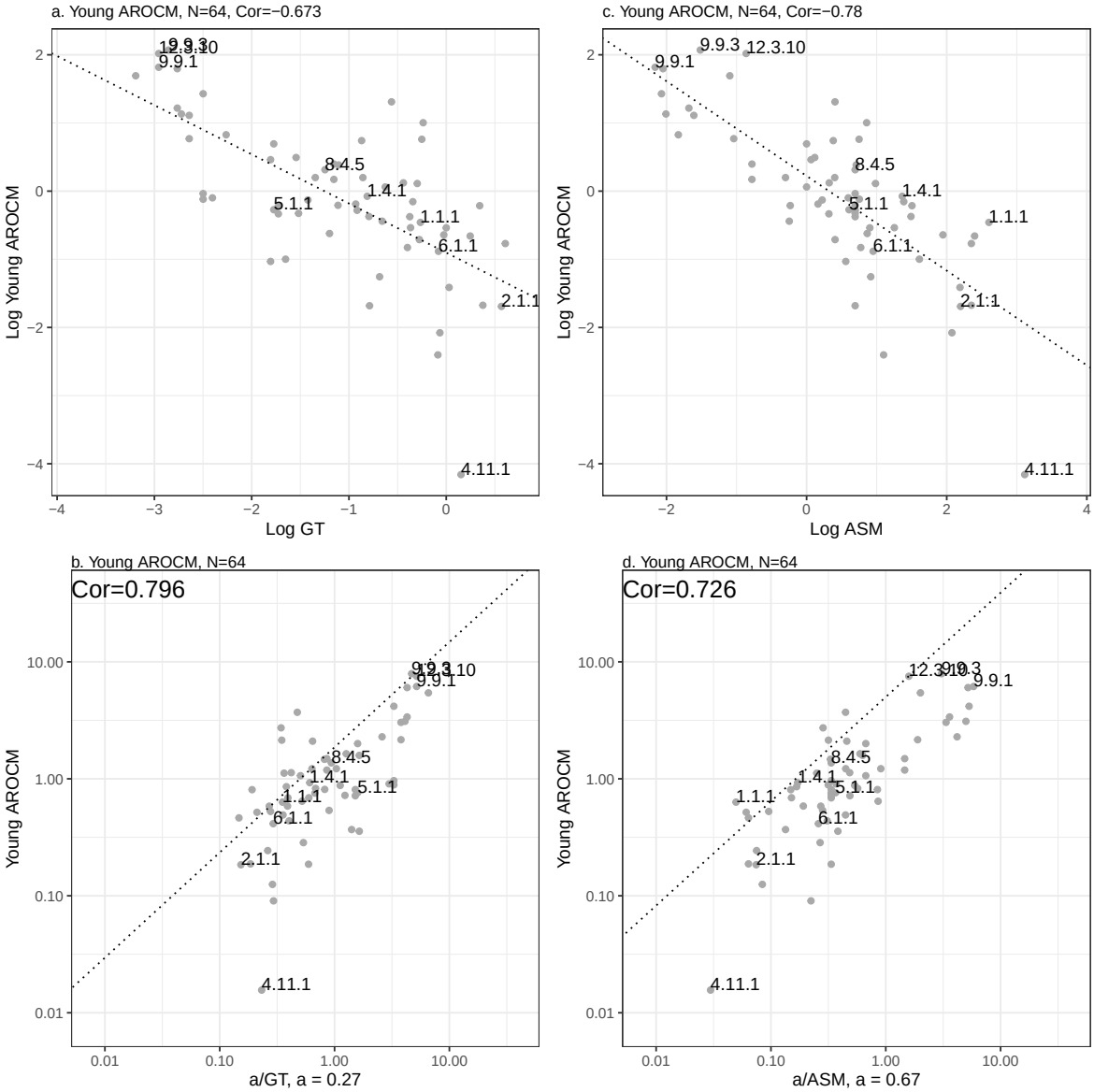

Figure S7: **AROCM in young animals versus gestation time**. Young AROCM$[0, 0.1L]$ vs. Gestational Time (GT, panels a,b) and Age at Sexual Maturity (ASM, panels c,d).

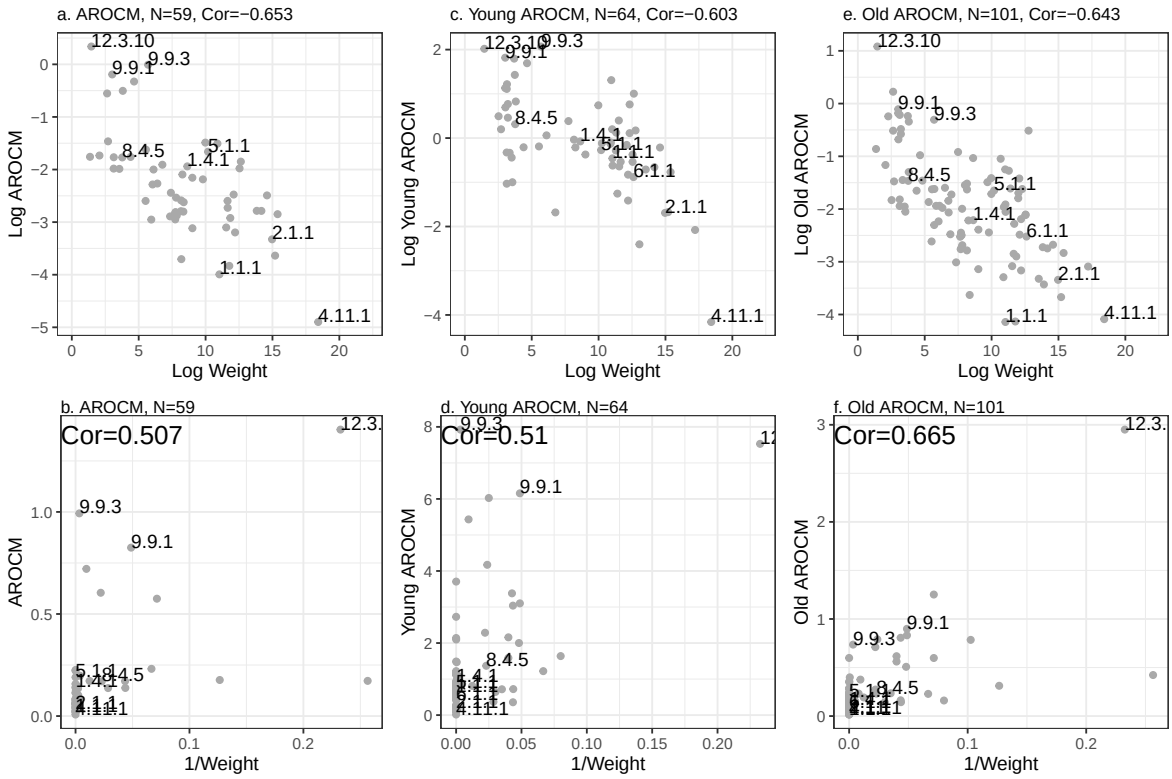

Figure S8: **AROCM versus average adult weight in different age groups**. Columns correspond to different age ranges: (a,b) all ages AROCM, (c,d) Young AROCM$[0, 0.1L]$, and (e,f) old AROCM. The first row panels (b,c,e) present log transformed AROCM (y-axis) against average adult weight (x-axis). The second row panels (b,d,f) contrast untransformed AROCM values (y-axis) with $1/Weight$ (x-axis)

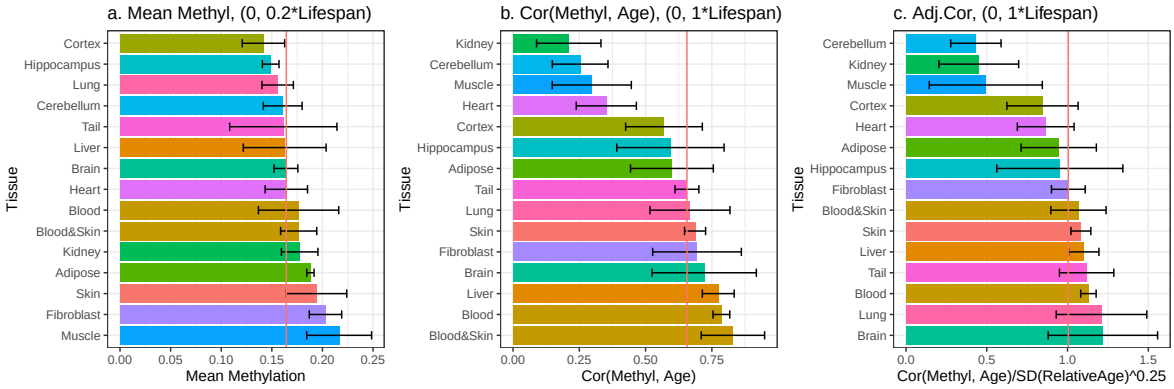

Figure S9: **Age correlations in different mammalian tissue types.** This figure depicts Mean Methylation, Cor(Methyl, Age), and Adjusted Cor in BivProm2+ across tissue types. Error bars signify 1 standard error from the median per tissue type, with the red vertical line indicating the overall median. Results, however, are confounded by species, prompting the use of multivariate regression models to explore tissue type effects (Table 1).

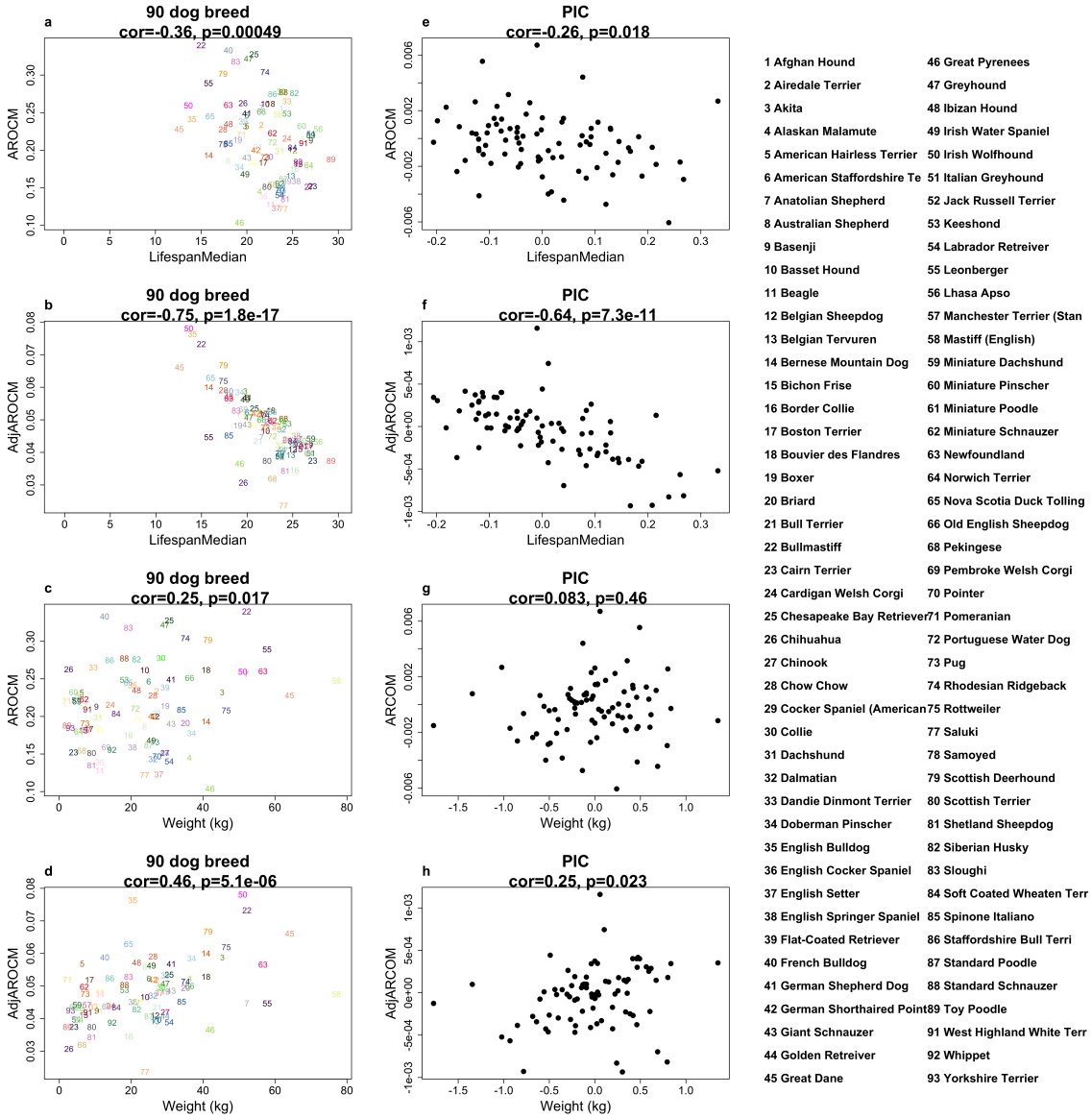

Figure S10: **Phylogenetic independent contrasts of AROCM in dog breeds.** Dog breed phylogenetic relationships were established as per [27]. The left panels (a,b,c,d) illustrate original variable relationships, while the right panels (e,f,g,h) present related results for phylogenetic independent contrasts (PICs, [18]). Accounting for these phylogenetic relationships via phylogenetic regression, both AROCM and Adj.AROCM retain significant lifespan correlations (e,f).

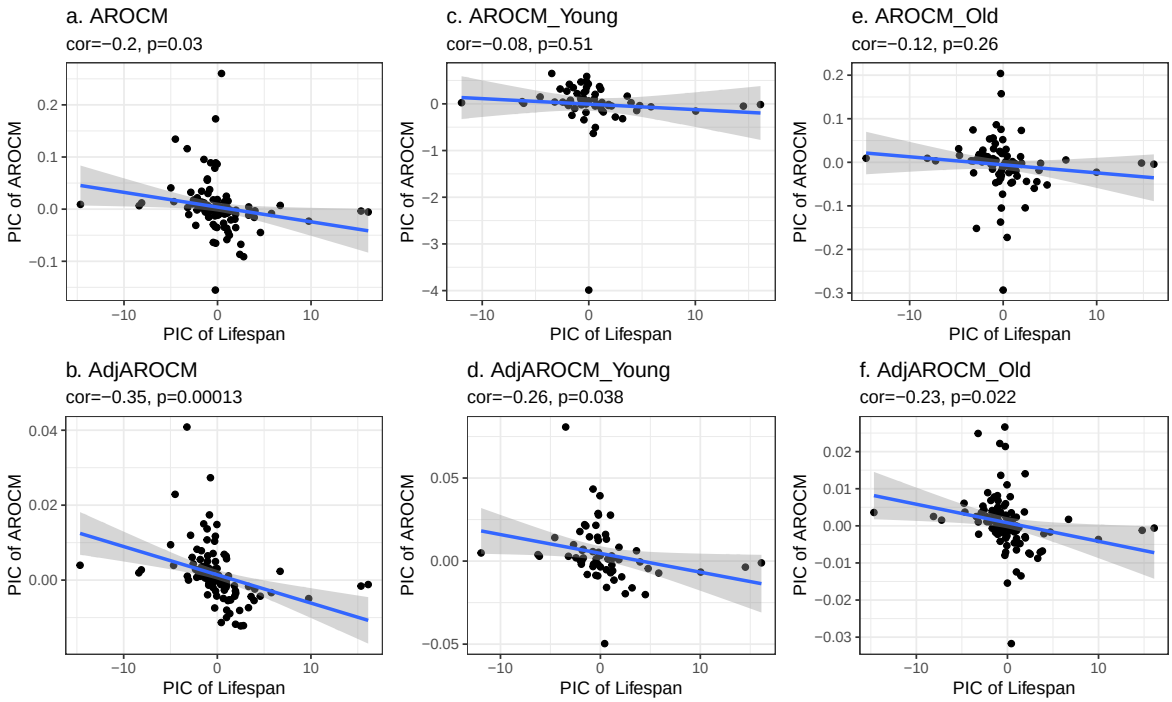

Figure S11: **Phylogenetic independent contrasts of AROCM in mammalian species.** The columns represent various age ranges: a,b) AROCM for all ages, c,d) young AROCM$[0, 0.1L]$, and e,f) old AROCM. The first and second row panels (a,c,e; b,d,f) show results for unadjusted and adjusted AROCM, respectively. Despite considering the phylogenetic links between mammalian species, the three adjusted AROCMs maintain significant lifespan associations. The phylogenetic relationships between species come from TimeTree [31].

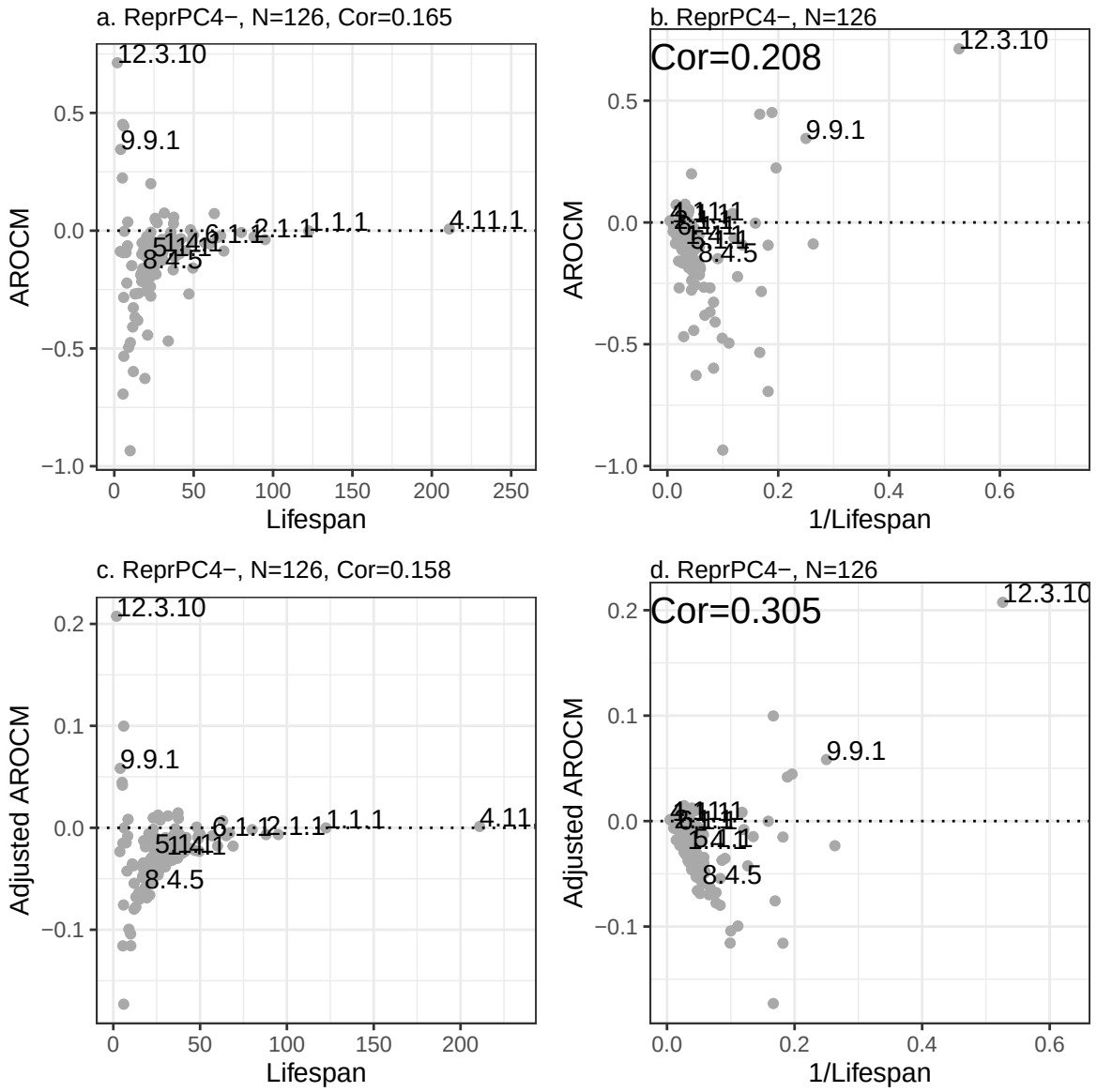

Figure S12: **Non-significant association between AROCM and Lifespan in some chromatin states.** Optimal power chosen to be 0.85 for ReprPC4-.

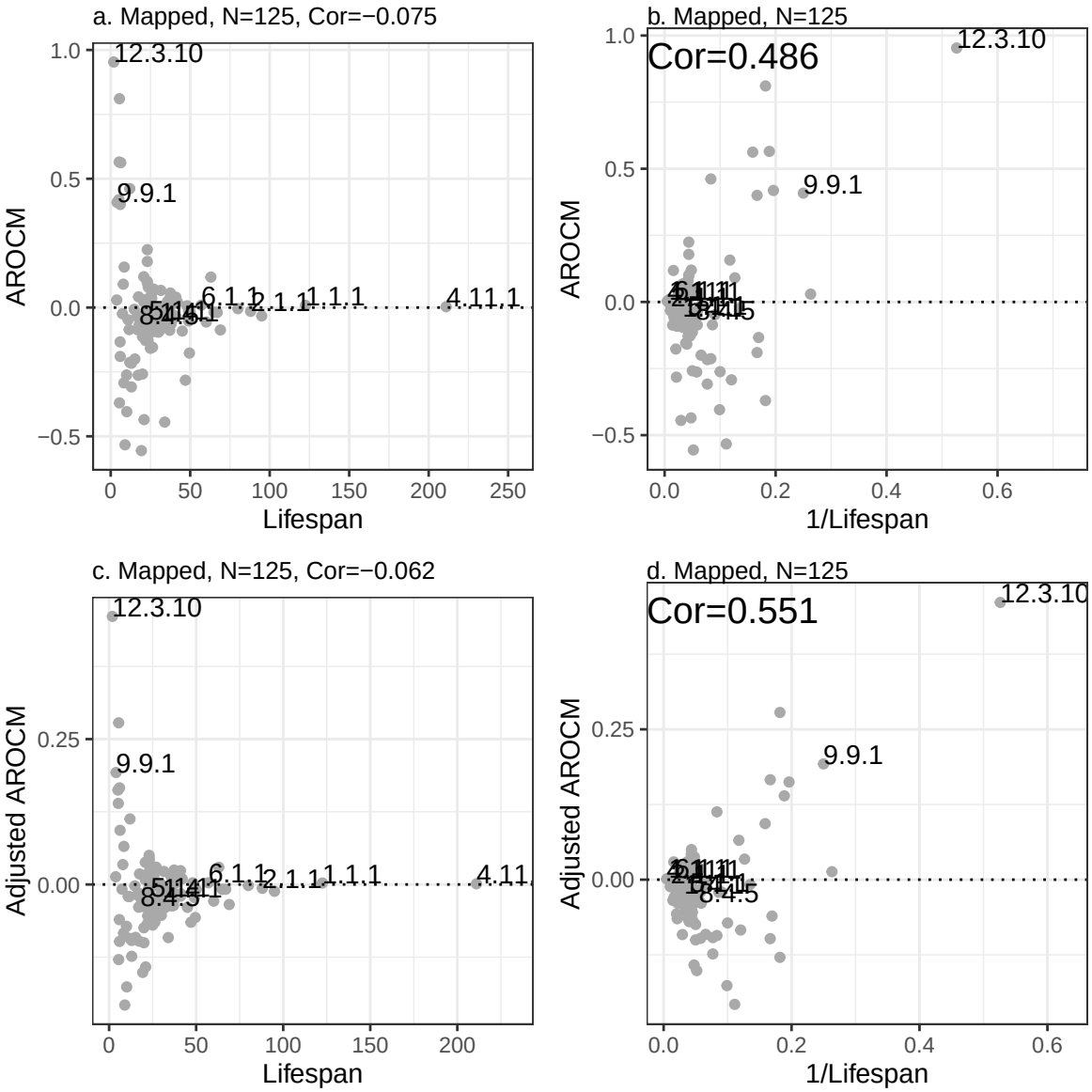

Figure S13: **Non-significant association between AROCM and Lifespan in all CpG sites mapped to Eutherians and Marsupials (p = 8970).** Optimal power chosen to be 0.5 for Adj.AROCM.

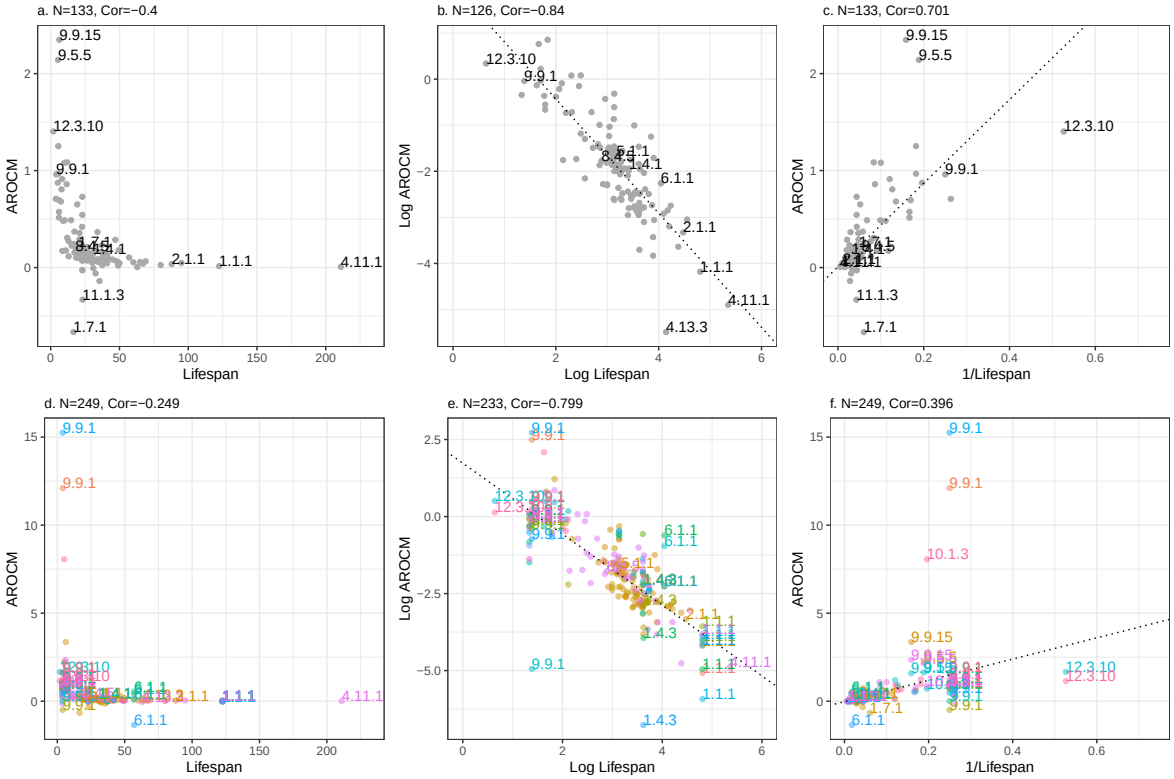

Figure S14: **AROCM versus Lifespan with outliers in mammalian data.** This figure is analogous to Figure 6 but with outliers not filtered by criteria 3 and 4 in Methods.